AD-A257 945

(11)

The Pennsylvania State University
APPLIED RESEARCH LABORATORY
P.O. Box 30
State College, PA 16804

DTIC
ELECTE
NOV 2 0 1992
S
C
D

EXPERIMENTAL ANALYSIS OF THE AEROACOUSTICS OF CASCADED AIRFOILS

by

L. A. Perry
G. C. Lauchle

Technical Report No. TR 92-08
November 1992

L.R. Hettche, Director
Applied Research Laboratory

92-29850

92

TABLE OF CONTENTS

DTIC Q

LIST OF FIGURES

LIST OF TABLES

Chapter 1

INTRODUCTION

The purpose of this study is to investigate the noise radiated by various louver designs. A louver is essentially a cascade of small airfoils, operating at the same angle of attack. Louvers are commonly used in heating, ventilation, and air conditioning (HVAC) systems to provide directional control of the exit airflow.

The HVAC system of an automobile can be a significant source of acoustic annoyance. Louvers are typically placed in the near field of the driver and passenger and can be major contributors to the overall interior noise level. In this study, thirteen representative dashboard registers used in automotive HVAC applications are considered. These registers vary in airfoil shape, number of airfoils, number of support struts, inlet and outlet sizes, and other physical parameters. The research documented in this thesis is directed toward a better understanding of the parameters that significantly affect the amount of noise generated by a louver.

1.1 Background and Research Objectives

In many applications, it is the trailing edge that is responsible for most of the noise radiation from small airfoils at low flow velocities. Sound generation from the trailing edge of an airfoil typically takes two forms: (1) tonal sound which is

associated with laminar flow over airfoils and (2) broadband noise which is due to the convection of upstream turbulent flow past the trailing edge.[1] The geometry of the leading and trailing edges and the angle of attack influence the type of flow over the surface, and therefore, the type of acoustic radiation emitted by the airfoil.

Turbulence in the inflow, wake, or turbulent boundary layer creates relatively inefficient quadrupole radiation; however, as this turbulence interacts with the leading or trailing edges of an airfoil, quadrupole source components of the turbulent pressure fluctuations are converted to more efficient dipole radiators.[2]

The Reynolds number (R_c) based on airfoil chord length, c, and free-stream velocity, U, is defined by Uc/ν, where ν is the kinematic viscosity of air. If R_c is smaller than 2×10^5, then the flow entering the trailing edge (TE) region will be laminar. At low R_c, laminar boundary layers develop whose instabilities result in vortex shedding and associated noise from the trailing edge. Vortex shedding will also occur in the small separated flow region downstream of a blunt trailing edge.[2] The noise from the trailing edge will be tonal in nature due to a Helmholtz instability in the periodic wake vorticity. The frequency of which maximum radiation occurs will scale as a Strouhal number. The Strouhal number is defined as: fl/U. The length scale, l, can be defined as δ, for sharp trailing edges or h, the trailing edge thickness for blunt terminations. As the angle of attack increases, local flow separation will occur on the airfoil and the tonal nature of the radiation disappears and the sound becomes broadband in character.[3]

The noise radiated from a cascade is more complicated than simply the sum of the emissions from N independent airfoils, where N is the number of foils in the cascade. The complication arises because of blade-to-blade interactions and increasing blockage (solidity) as N gets large. The turbulence structure over the individual blades may be altered as the solidity increases, which will have an effect on the aerodynamic noise produced.

Registers are used in automotive HVAC systems to control the amount and direction of air flow. Registers are typically made up of a louver installed in a plastic housing. The housing provides an aesthetically pleasing mount for the louvers and may also be equipped with an air shut-off door to further control the amount of flow. Structural support struts for the louvers may be placed in front of the louvers. The number of louvers and shape of the airfoils in the cascade vary. Louvers may have two sets of cascades (dual vane), placed at 90° to each other, to provide control of the flow in two directions.

The primary objective of this study is to determine the spectrum of radiated noise from the registers under various independent operating conditions (e.g. free-stream velocity, number of airfoils, and airfoil shape). This is applied research with a goal of understanding the sound generating mechanisms well enough, so that noise control methods can be implemented. The interpretations and conclusions are based on only one angle of attack, zero degrees.

1.2 Organization of Thesis

Chapter 2 describes the facility and instrumentation used to measure the noise radiated by the louvers. The data acquisition and signal processing procedures, along with computer based programs used to process the data, are reported. Validation properties of the facility are reported in the form of open jet data and signal-to-noise measurements.

Chapter 3 contains physical descriptions of the registers along with the results of the acoustical measurements. The acoustical measurements are presented in the form of Power Spectral Densities (PSD) and Overall Sound Pressure Levels (OASPL).

In Chapter 4 the experimental data from Chapter 3 are interpreted. Scaling laws and correlations between the acoustics and the physical parameters of the registers are established. Conclusions and recommendations for further testing are presented in Chapter 5.

Chapter 2

EXPERIMENTAL PROCEDURE

The experimental setup is described in detail in this chapter. The electronic hardware used and the measurement procedures employed are fully documented, including sensor calibration and digital data acquisition and processing techniques. Signal-to-noise measurements and open jet data are reported for the facility validity check.

2.1 Description of the Facility

Figure 2.1 shows a sketch of the experimental set-up. Testing was conducted in the ARL Penn State Flow-Through Anechoic Chamber. The anechoic chamber is reflection free down to 70 Hz.[4] A portable wire mesh floor was designed to support the test apparatus above the fiberglass wedges located on the ground floor.

Airflow is supplied by a 20 HP centrifugal blower situated outside the anechoic chamber and contained within a sound isolation box. The inlet to the blower is acoustically treated by use of a commercial muffler. As sketched in Figure 2.1, a 4 inch flexible air hose connects the air source to another plenum box inside the anechoic chamber. This plenum box eliminates all turbulence in the approach

5
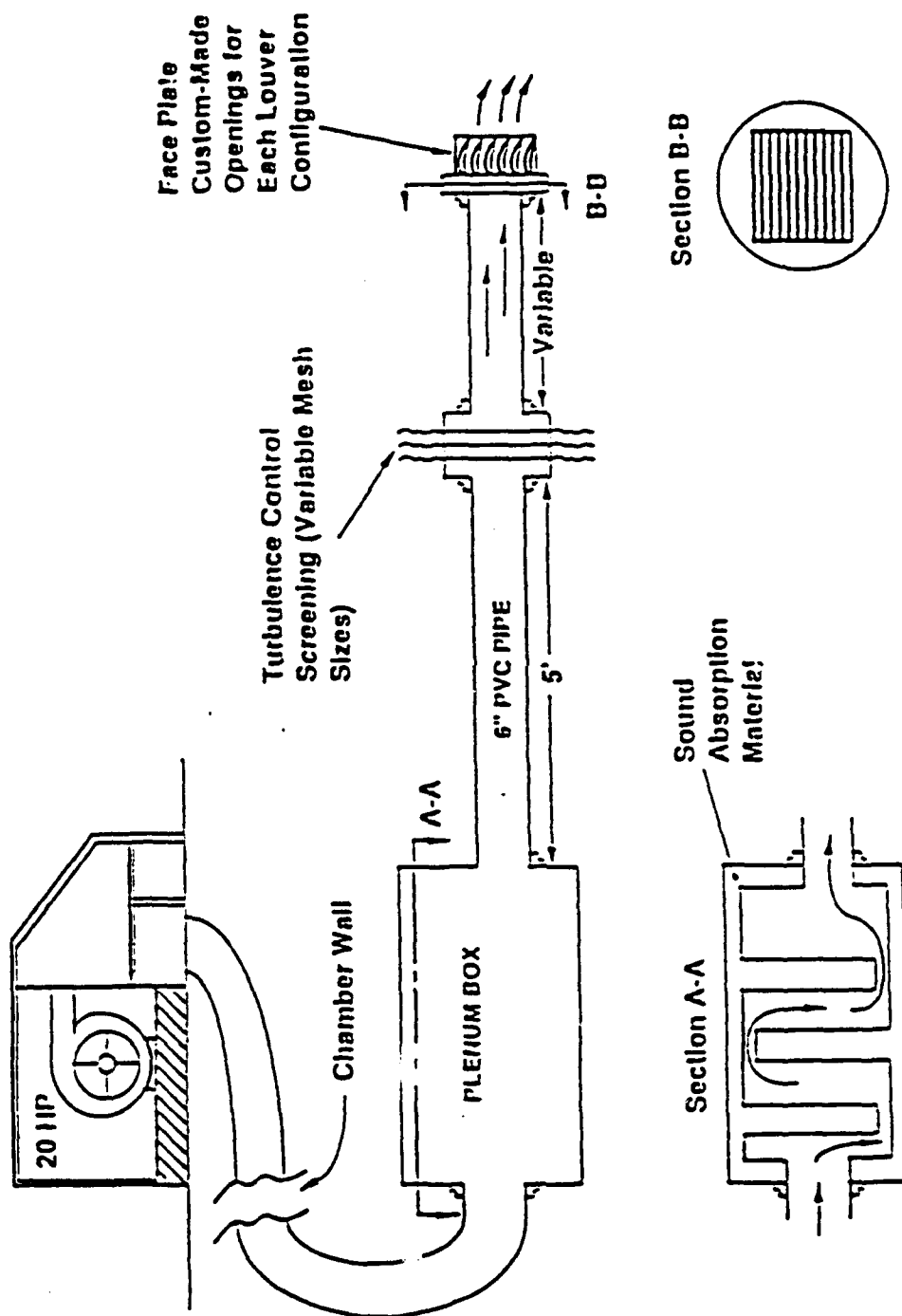
Figure 2.1   Experimental Test Set-up.

stream (due to its large volume) and provides two acoustically-treated baffles to attenuate the blower noise.

At the exit of the plenum box, investigators have the option of placing the louver vent directly within the opening (circular orifice), or adding pipe and turbulence screens for the study of turbulence ingestion noise. For this study, the louvers were placed directly within the plenum exit orifice. Each louver had a separate face-plate form fitted to its contours. This face plate was bolted onto the plenum box, over the exit orifice.

The blower speed is controlled by a three-phase inverter, allowing flow velocities at the plenum exit to be set to any value between 4.9 and 34 m/s. Inlet flow velocities provided to the louver designs were based on typical automotive operating conditions. Seven inflow velocities were chosen to determine scaling relationships and limit the scope of the experiment. These seven velocities are as follows: 5.17, 5.73, 6.27, 6.81, 7.35, 7.89, and 8.43 m/s. The velocity is measured with a Pitot-static pressure probe. The flow rates were established from probe scans across the open jet orifice without the louver installed.

2.2 Instrumentation

A 1/2 inch B&K microphone (Type 4133) was situated 45° off the centerline of the exit and at 1 meter from the plane of the register. 40 dB of amplification

was provided by an Ortec Differential AC Amplifier (Type 9454). A B&K piston phone (Type 4220), which produced a level of 124 dB at 250 Hz at the face of the microphone, was used to calibrate the microphone.

A Whittaker Corporation pressure transducer (Model KP15) was used to measure the change in pressure sensed by the pitot tube. The pressure transducer provided a DC voltage output to the data acquisition device. A computer program was used to apply a calibration value to the DC voltage converting it to a change in pressure. Bernoulli's equation was then applied to determine the air flow velocity, measured at the plenum exit, in m/s.

2.3 Data Acquisition and Processing

Acoustic data acquisition was performed using a Zonic A&D, Inc,. System 7000, 8-channel parallel signal processor. A VAXstation 3100 computer controlled the processor and performed the spectral computations using the Zonic Engineering Test Analysis software (ZETA). Data were taken at a 12.8 kHz sampling rate which provides for spectral estimates up to 5 kHz. A Hanning window was used for spectral smoothing. Two hundred and fifty-six ensembles with a 50% overlap were used in the spectral averaging. The effective analysis bandwidth (B_e) was 6.25 Hz.

Power spectral densities (PSD) were estimated by using 800 point Fourier transforms. The PSDs computed by ZETA were saved onto a 3 1/4" floppy disk for later analysis using Fortran based computer programs. The overall sound pressure levels (OASPL) were calculated by performing an integration over the frequency bins of interest.

The effective bandwidth (B_e) and the number of averages (n_d) can be used to assess the statistical accuracy of the spectral measurements. According to Bendat and Piersol,[5] the normalized random error is expressed as: $e_r = (1/n_d)^{1/2}$. The bias error is negligible for $B_e = 6.25$ Hz, unless pure tone components are present in the data. No pure tones were observed in the data acquired.

A Fortran program written by a Penn State student, Paul Bent, is used to interpret the acquired spectra. This program uses a method described by W. Neise,[6] which uses the similarity laws for centrifugal fans developed by J. Weidemann.[7] The program separates the autospectrum into two components: G(He) and F(St), where G(He) is an acoustic response function which depends on the geometry and structural makeup of the system under study. This function includes acoustic scattering and its dependence on Helmholtz number, He. The Helmholtz number is defined as: fl/c. Where c is the speed of sound. The function F(St) is the source spectral distribution function which depends on free-stream velocity through the Strouhal number, St. The algorithm extracts Strouhal effects from the spectra allowing for an easier interpretation of the results. The Appendix contains the Fortran code used along with additional information on the procedure.

2.4 Facility Validation

Figure 2.2 contains the PSDs at the 7 different flow velocities with no louver at the exit of the plenum box. This open jet data scales to the 5.3 power of velocity, based on overall levels. This scaling relationship is indicative of noise radiated from a laminar flow nozzle.[8] Figure 2.3 is a comparison of the PSDs of the open jet spectra and the spectra with a representative register (number 5) installed in the exit orifice. A 10 dB signal-to-noise ratio is apparent for frequencies above 200 Hz. This signal-to-noise ratio is consistent for all the louvers tested. The large energy band at very low frequencies (below 500 Hz) is velocity dependent and is basically jet or facility induced. This band of energy persists in the measured spectra regardless of the number or geometry of the blades installed in the housing, and is therefore considered unrelated to the aeroacoustics of the louvers under study.
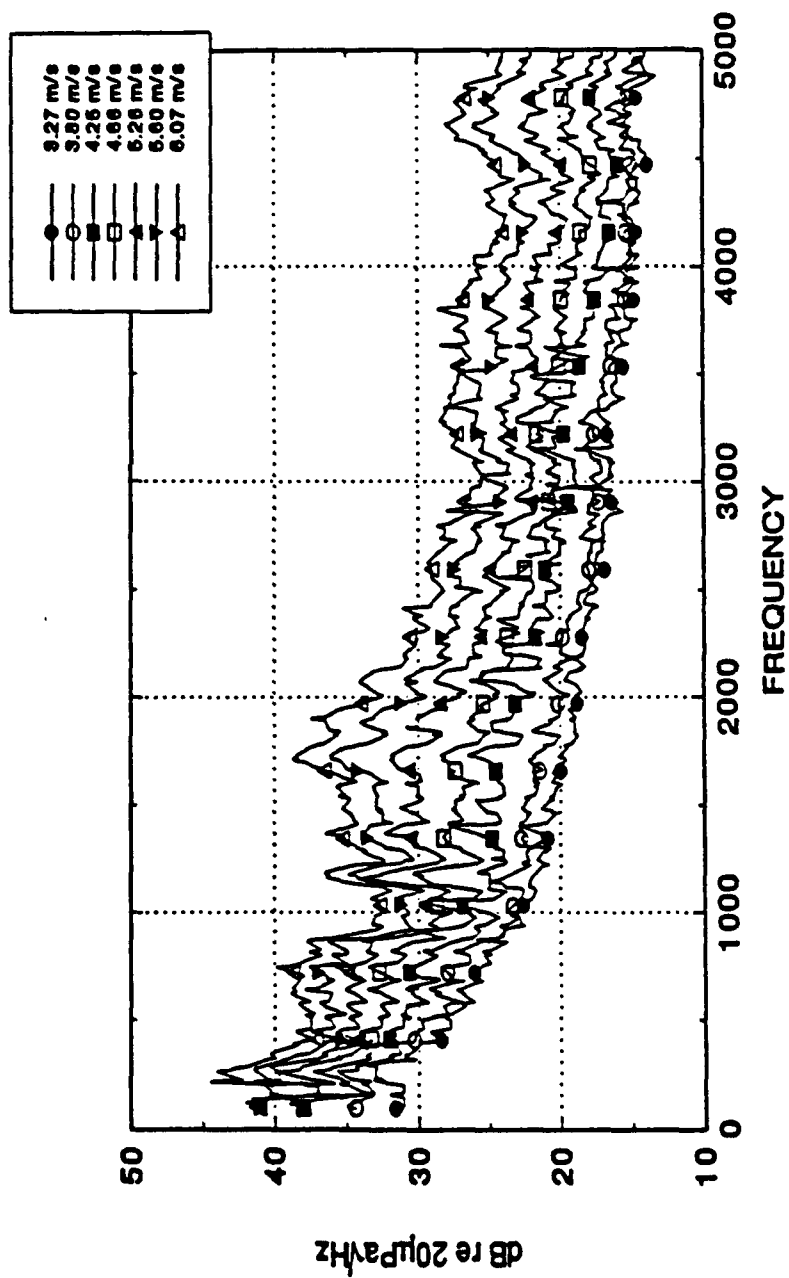
Figure 2.2   PSDs Acquired for the Open Jet.
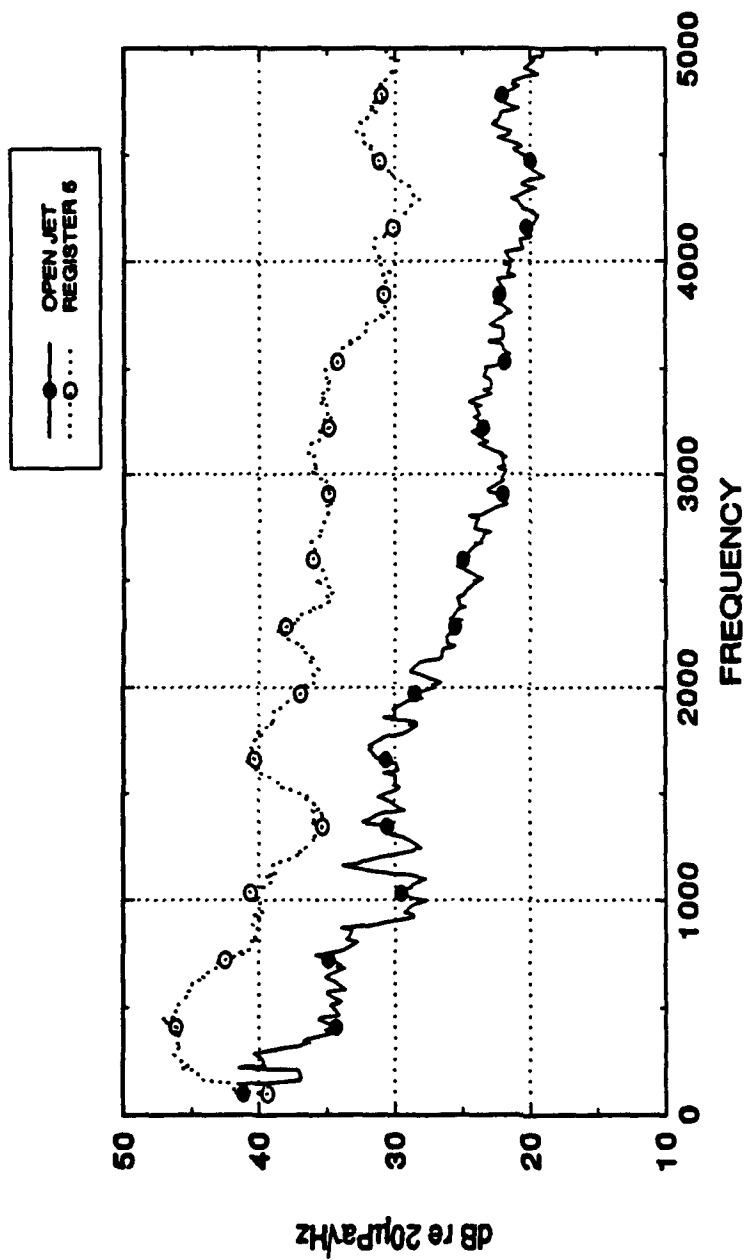
Figure 2.3   Comparison of Spectra Acquired From the Open Jet and Register 5 at 5.26 m/s.

Chapter 3

EXPERIMENTAL RESULTS

For each of the registers evaluated, the experimental results are presented in the form of Power Spectral Densities (PSDs) of the radiated sound pressure at the measurement location, 1 meter from the face of the register and 45° off the centerline of the exit. The spectra were acquired at seven different inflow velocities, typical of automotive applications. The stock configuration was evaluated for each register. Additional configurations were tested for register numbers 2, 3, 5, 8, 10, and 20. Modifications were made to the number and shape of the airfoils and the condition of the shut-off door and housing. The results of the multi-configuration tests are presented first. The data acquired for the registers that remained unmodified are presented at the end of the chapter. A photographic representation of each register is provided along with a description of pertinent physical parameters.

From the 30 automotive registers supplied by the sponsor, 13 were selected based on their unique differences, and on the ability to mount them in the test fixture. This explains the non-sequential numbering of the registers. Table 3.1 is a listing of the registers and some of their physical parameters including inlet/outlet area, leading and trailing edge thicknesses, chord and span lengths.

Table 3.1   Physical Parameters of the Registers.

NO.	DESCRIPTION	VANES	STRUTS	OUTLET /INLET AREA (cm²)	VANE/STRUT DIMENSIONS (mm)			
					SPAN	CHORD	THICKNESS	
							T.E.	L.E.
2	DUAL VANE	7	5	57.75 48.98	73.0 73.0	15.0 16.0	0.5 1.5	3.0 2.0
3	BARREL	7	2	46.20 51.70	42.0 112.0	22.0 7.0	0.5 2.0	3.0 2.0
5	CIRCULAR	4	0	52.80	82.0	26.0	2.0	2.0
7	DUAL VANE	5	5	63.75 19.25	42.0 83.0	17.0 15.0	3.0 2.0	3.0 2.0
8	DUAL VANE	6	5	63.13 61.36	58.0 100.0	19.0 17.0	1.0 1.5	1.0 2.0
9	DUAL VANE	5	5	51.00 62.90	75.0 58.0	14.0 18.0	3.0 3.0	3.0 3.0
10	BARREL	7	2	44.80 54.61	22.0 114.0	37.0 8.0	2.0 3.0	3.0 3.0
14	BARREL	3	6	51.00 51.00	70.0 60.0	23.0 20.0	2.0 2.0	2.0 2.0
15	BARREL	5	0	24.00 24.00	30.0	17.0	1.0	1.0
16	BARREL	10	2	49.14 49.14	30.0 107.0	20.0 8.0	1.0 1.0	3.0 1.0
17	BARREL	3	2	26.68 26.68	58.0 42.0	21.0 13.0	0.5 2.0	2.0 2.0
20	SQUARE BARREL	3	3	26.00 42.24	50.0 50.0	25.0 12.0	2.0 2.0	3.0 2.0
30	BARREL	5	0	20.44 20.44	27.0	16.0	1.0	1.0

3.1 Register 2

Register 2 is a dual vane type of register, meaning both the vertical and horizontal airfoils are adjustable. The register has an air shut-off door consisting of two rectangular pieces of plastic with a thin piece of acoustic foam between them. The rearmost airfoils have blunt leading and trailing edges. The forward airfoils have blunt leading edges and very sharp trailing edges. Figure 3.1 is a photograph of this register. The register was evaluated with and without the shut-off door.

Figure 3.2 are the PSDs acquired for the stock register and Figure 3.3 are the PSDs of the register with the shut-off door removed. Both sets of data scale to the 6.6 power of velocity. Figure 3.4 is a comparison of the two configurations at an inflow velocity of 5.26 m/s. It can be seen that the shut-off door causes an increase of 3 to 5 dB in the energy bands centered around 1300 and 4300 Hz. However, removing the door caused a velocity independent peak to shift from 2100 Hz to 2500 Hz.

3.2 Register 3

This register is a barrel type. It has seven airfoils and two support struts. It has an air shut-off door consisting of two plastic pieces with acoustic foam between
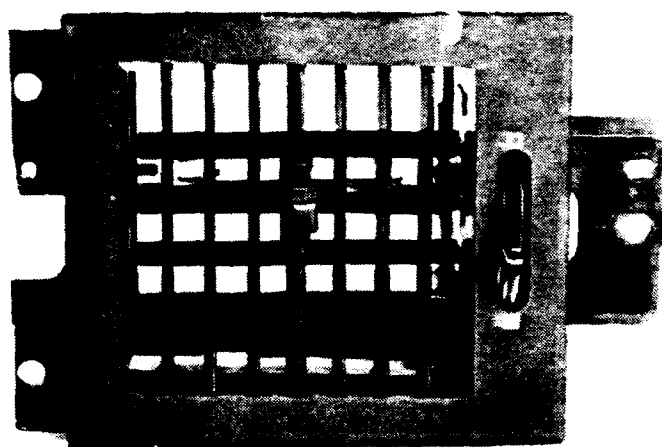
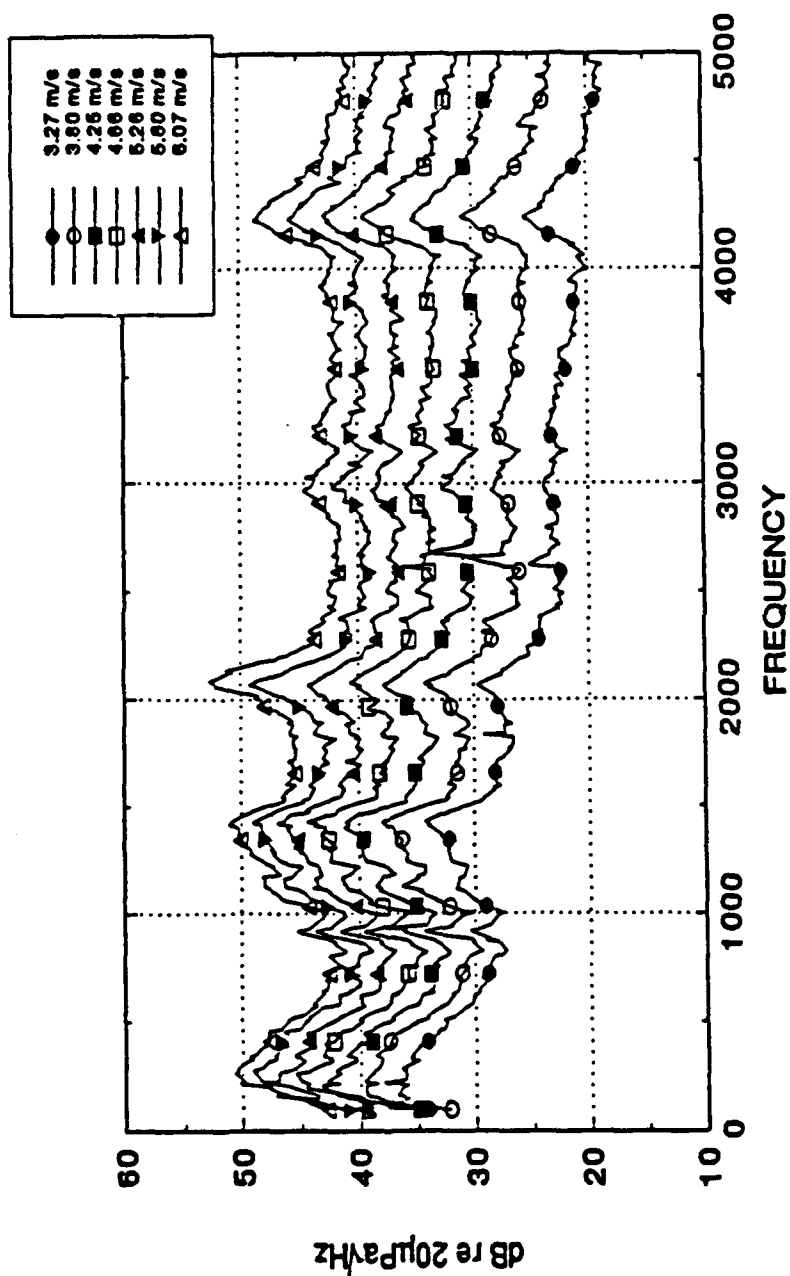**Figure 3.1** Photograph of Register 2.

Figure 3.2   PSDs Acquired for Register 2 - Stock Configuration.
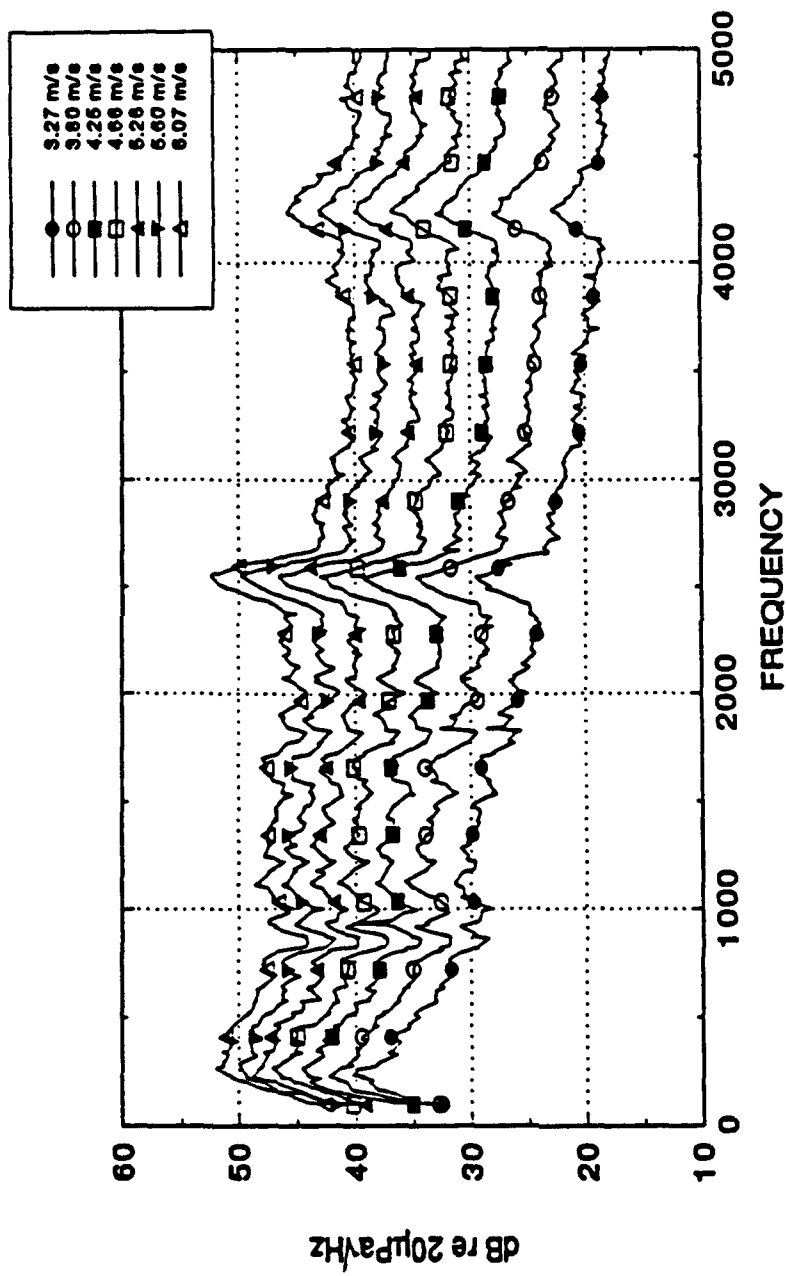
Figure 3.3   PSDs Acquired for Register 2 - Shut-off Door Removed.

Figure 3.4   PSDs Acquired for Register 2 - With and
              Without Shut-off Door at 5.26 m/s.

them. The shut-off door also has a rectangular cavity on each side. The airfoils have blunt leading edges with a notch and very sharp trailing edges. The struts have blunt leading and trailing edges of the same width (2 mm). Figure 3.5 is a photograph of this register.

Eight configurations were evaluated: (1) Stock, (2) Stock - without shut-off door, (3) Stock - with shut-off door with cavities filled in, (4) Housing only - with shut-off door, (5) Housing only - without the shut-off door, (6) Louver only, (7) Louver only, leading edge smoothed.

The spectra of the stock register scales to the 6.0 power of velocity. An obvious velocity dependent peak is apparent from 400 to 600 Hz for the stock configuration of the register (Figure 3.6). This peak disappears when the shut-off door is removed (Figure 3.7). Figure 3.8 contains the F(St) function calculated for the stock register using the thickness of the shut-off door as the length scale. The velocity dependent peaks collapse to a Strouhal Number of 0.22. Figure 3.9 is a comparison of the spectra of the stock register with and without the shut-off door and with the cavity in the door filled in. As shown, filling the cavity on the door shifts the velocity dependent peaks to higher frequencies, causing a shift in Strouhal Number to 0.28 based on door thickness. Figure 3.9 also indicates that overall, the stock register is the quietest of the configurations tested.

Figure 3.5   Photograph of Register 3.

Figure 3.6   PSDs Acquired for Register 3 - Stock Configuration.

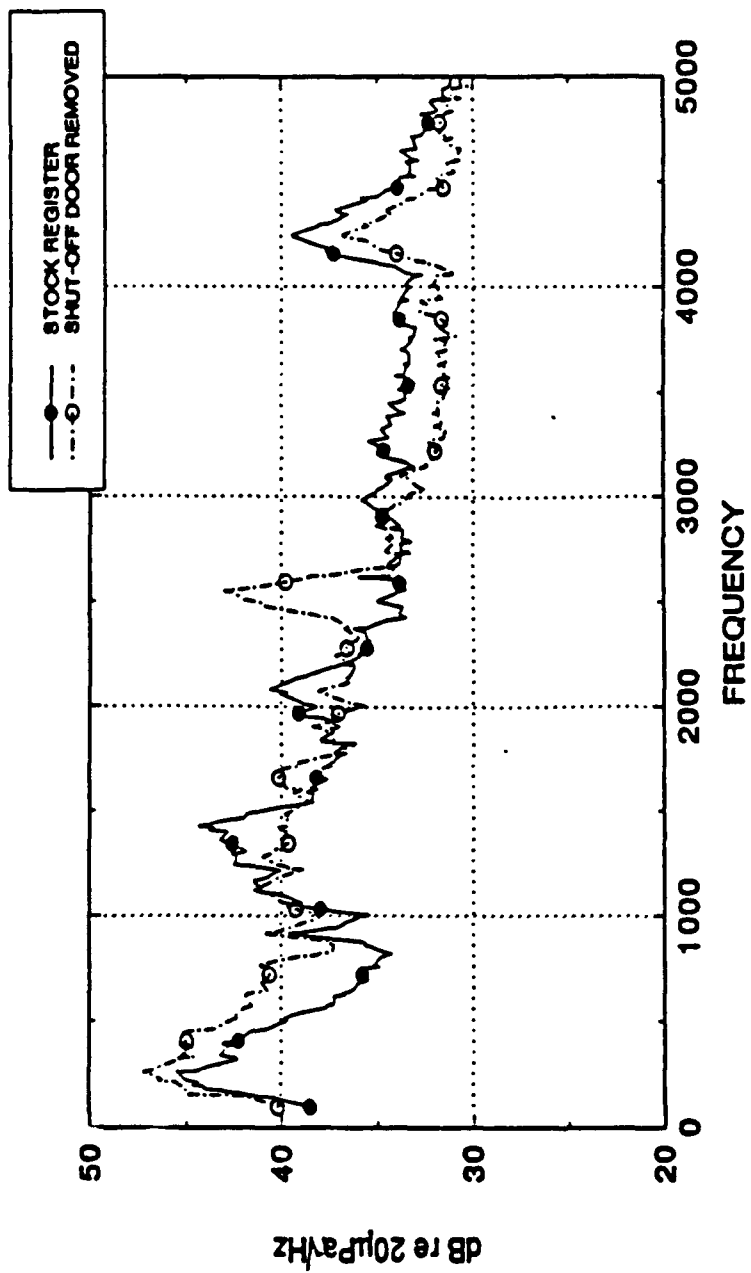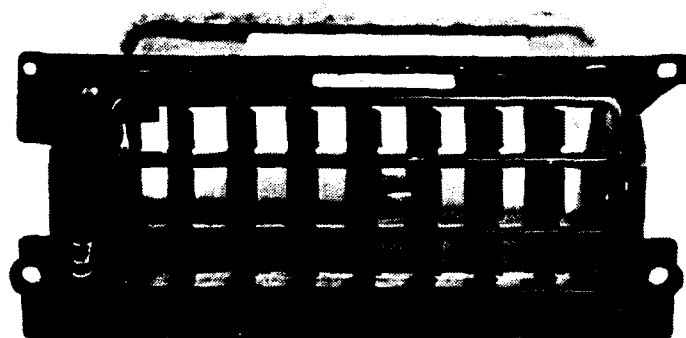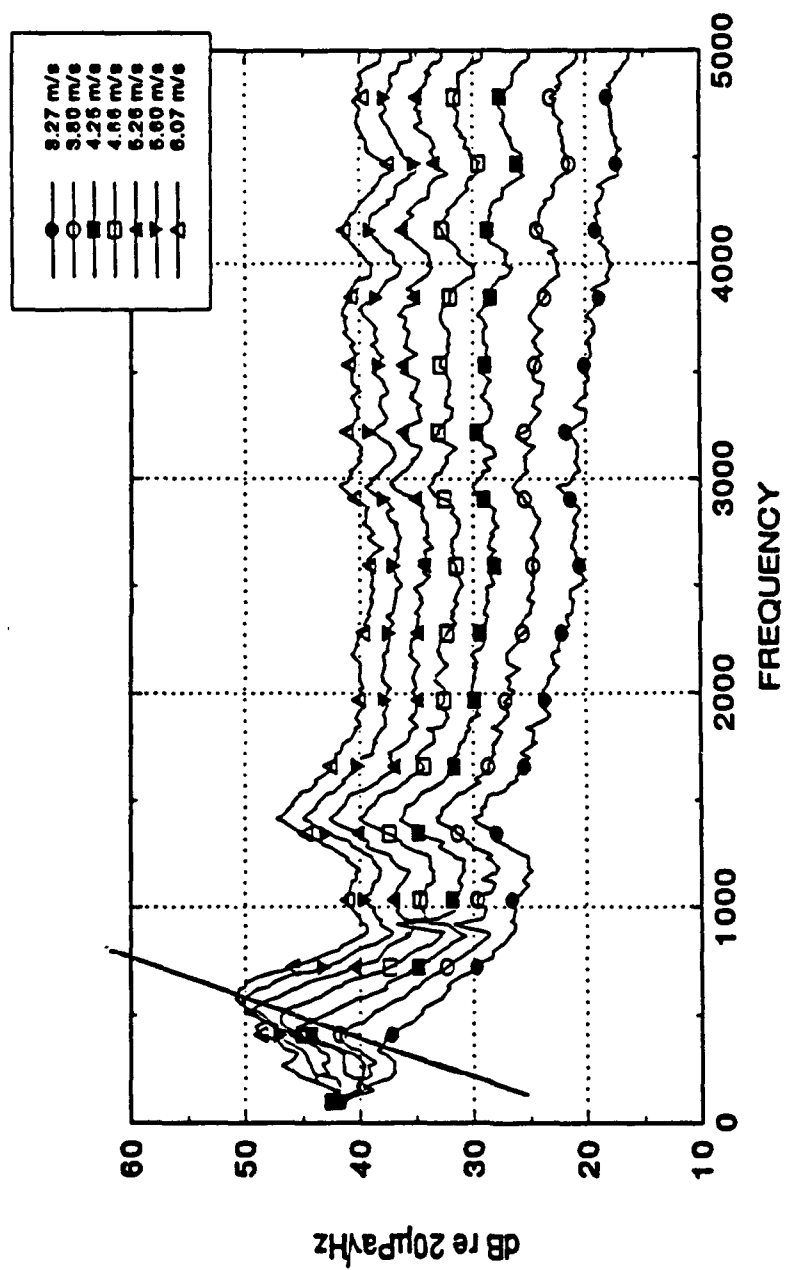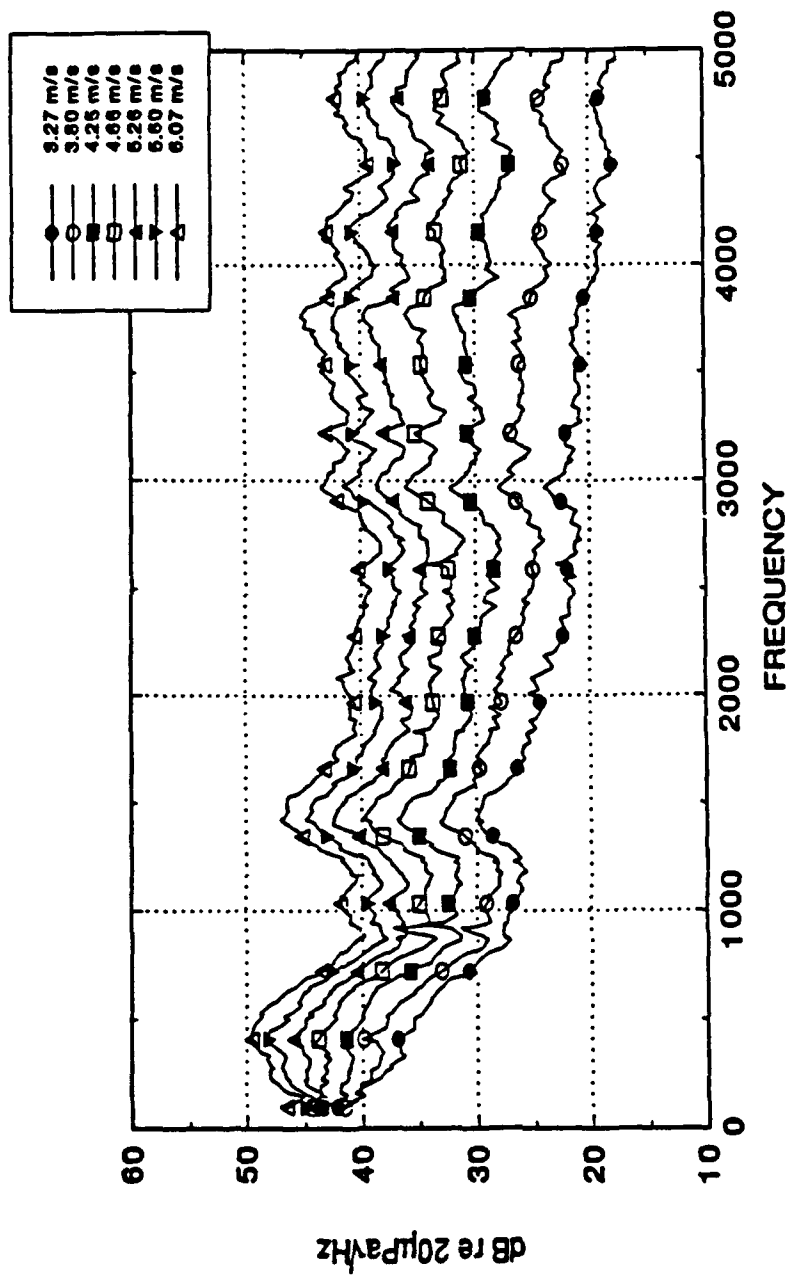**Figure 3.7**   PSDs Acquired for Register 3 - Shut-off Door Removed.
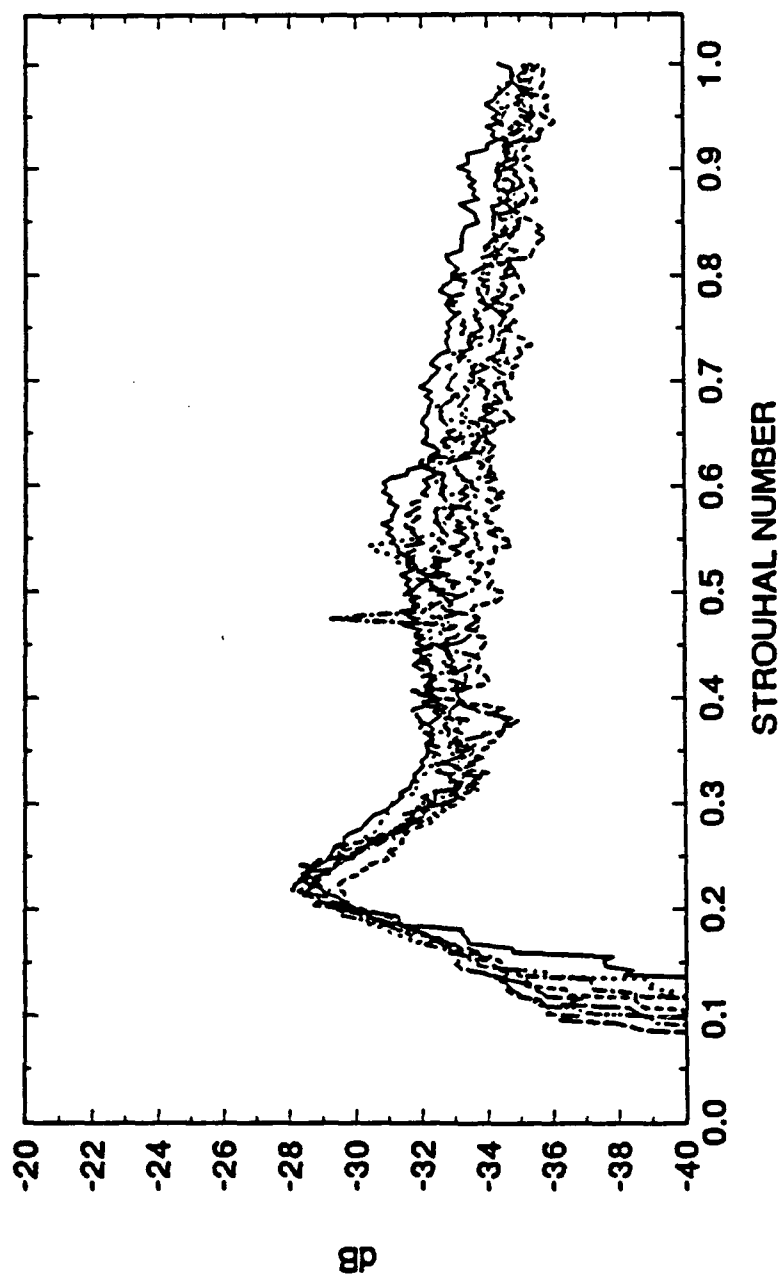
Figure 3.8   F-Function for Register 3 - Stock Configuration.
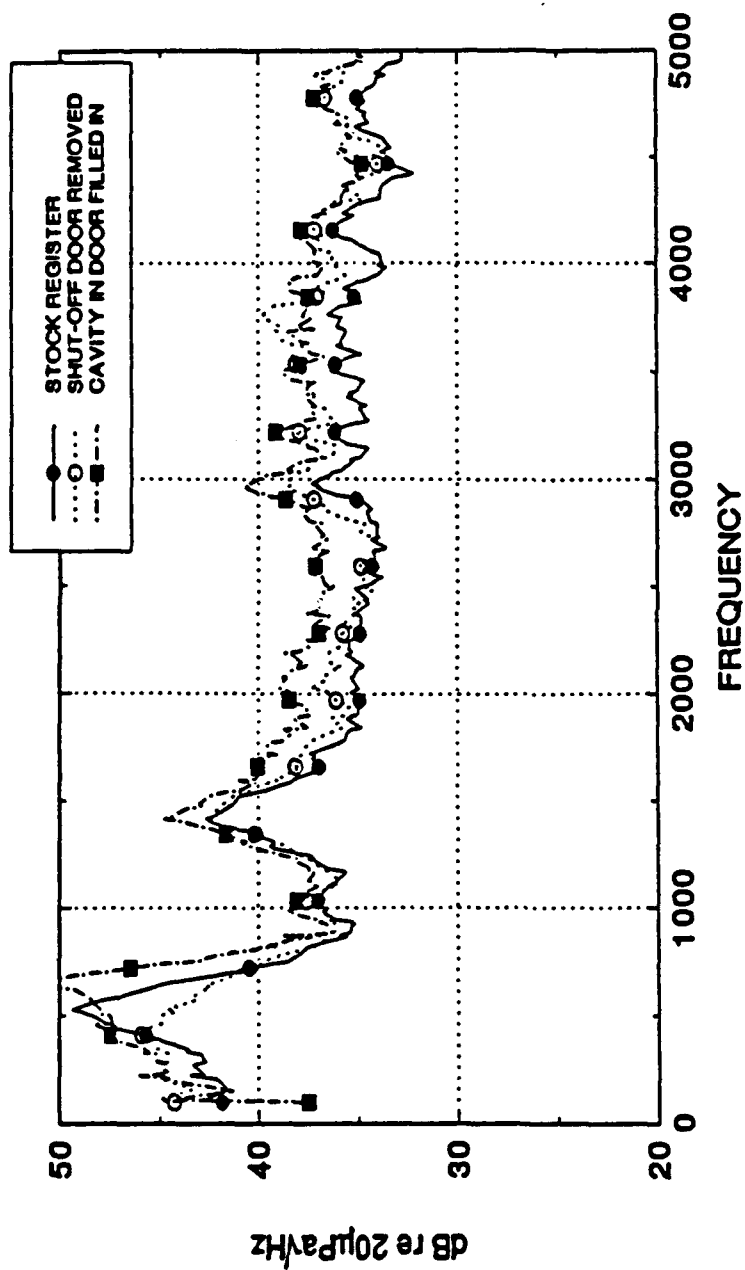
Figure 3.9   PSDs Acquired for Register 3 - Stock, Shut-off Door Removed, and Cavity in Shut-off Door Filled In at 5.26 m/s.

Figure 3.10 contains the spectra acquired with the louver, without the housing, installed in the test fixture. This was done by using a different face plate which conformed to the louver's contours. This difference in inlet area increased the velocity of the airflow over the airfoils. These data scale to the 6.0 power of velocity. Figure 3.11 compares the stock louver acoustic signature to the one acquired when the leading edges of the airfoils are smoothed. The smoothing of the leading edges results in 1 to 2 dB noise reduction, except at very high frequencies. Figure 3.12 compares the spectrum of the housing only to that of the louvers only and the stock register. The housing generates noise that is consistently 8 to 10 dB lower than the stock configuration. The addition of the housing increases the inlet area causing a decrease in the airflow over the blades, which reduces the noise generated by the louvers.

3.3 Register 5

Figure 3.13 is a photograph of register 5. A tie rod connects the four airfoils together so that they pivot together through common angles. When the airfoils are closed (90° angle of attack), each airfoil nests within steps molded in the adjacent airfoil. Therefore, three of the four airfoils have a forward and rearward facing step. A schematic of these airfoils is presented in Figure 3.14. The bottom most airfoil is flat except for a "thumb tread" molded onto its surface. This tread consisted of six ridges 1 mm high, spaced 2 mm apart.
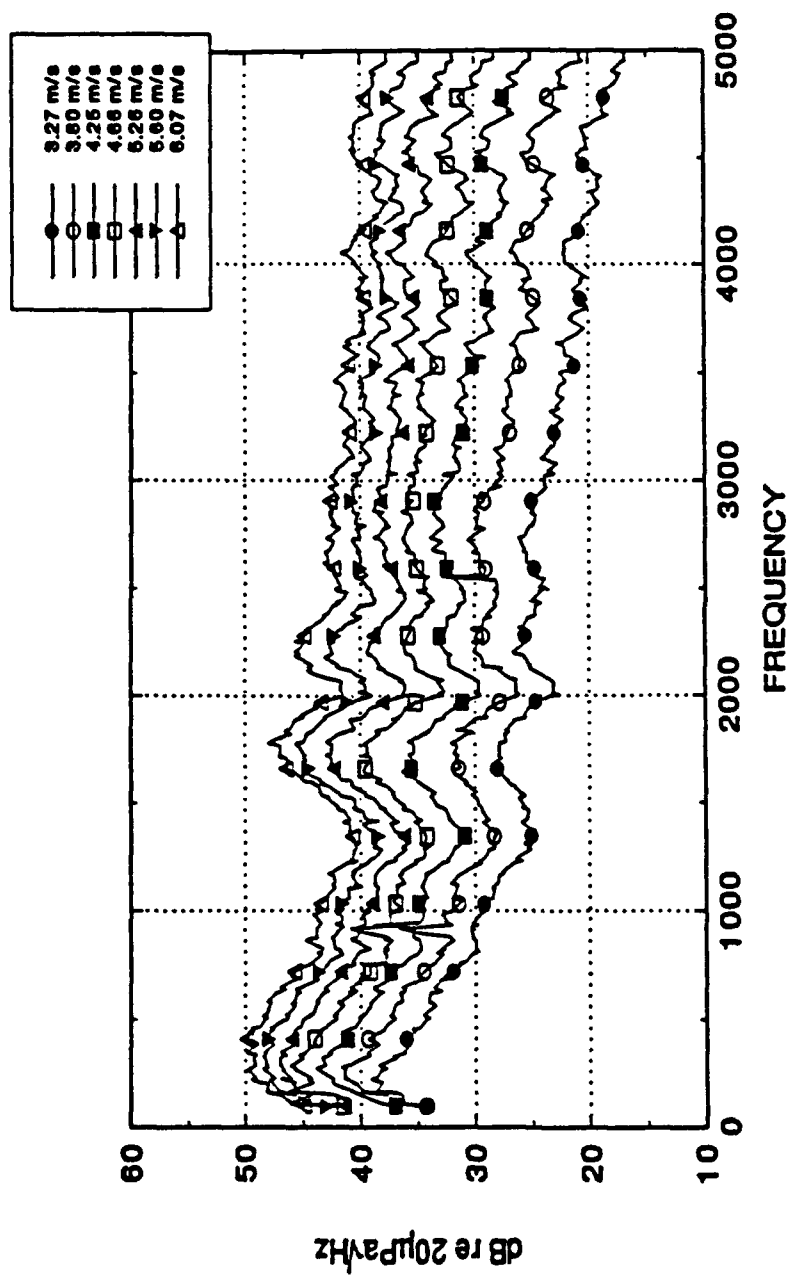
Figure 3.10   PSDs Acquired for Register 3 - Louver Only.
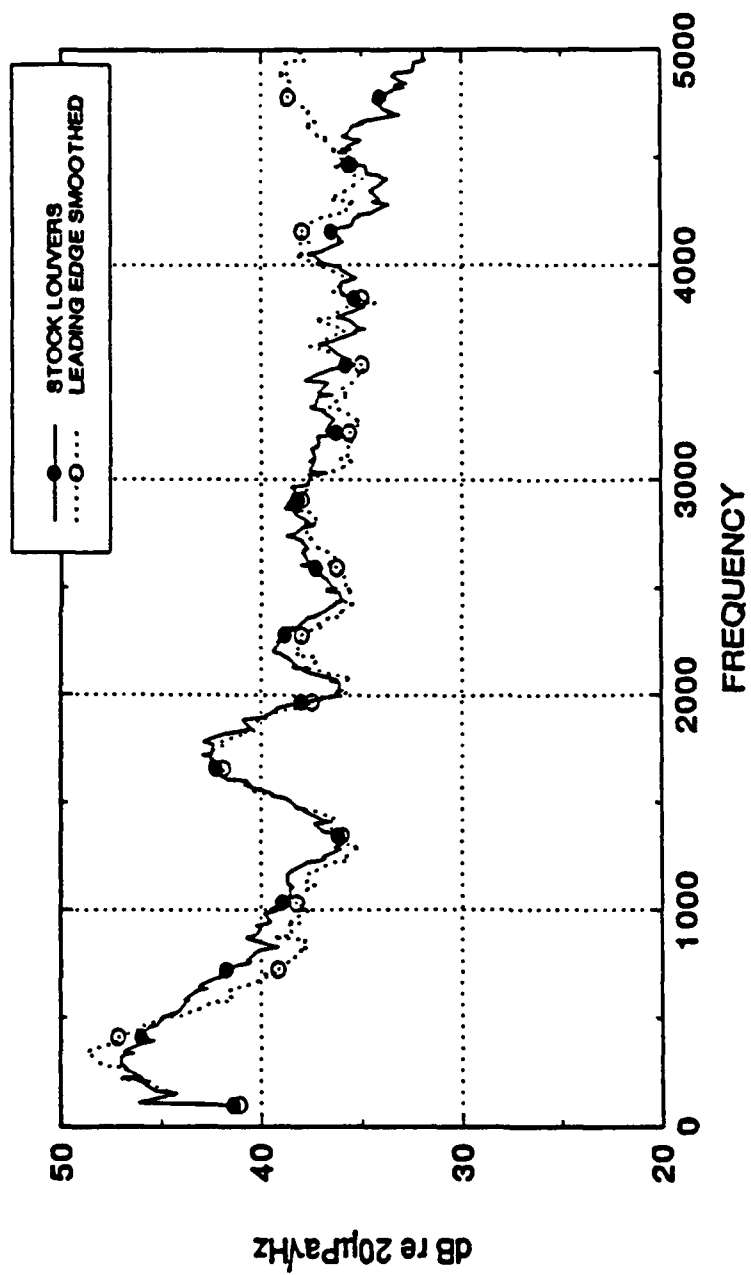
Figure 3.11   PSDs Acquired for Register 3 - Stock Louvers and Louvers with the Leading Edge Smoothed at 5.26 m/s.
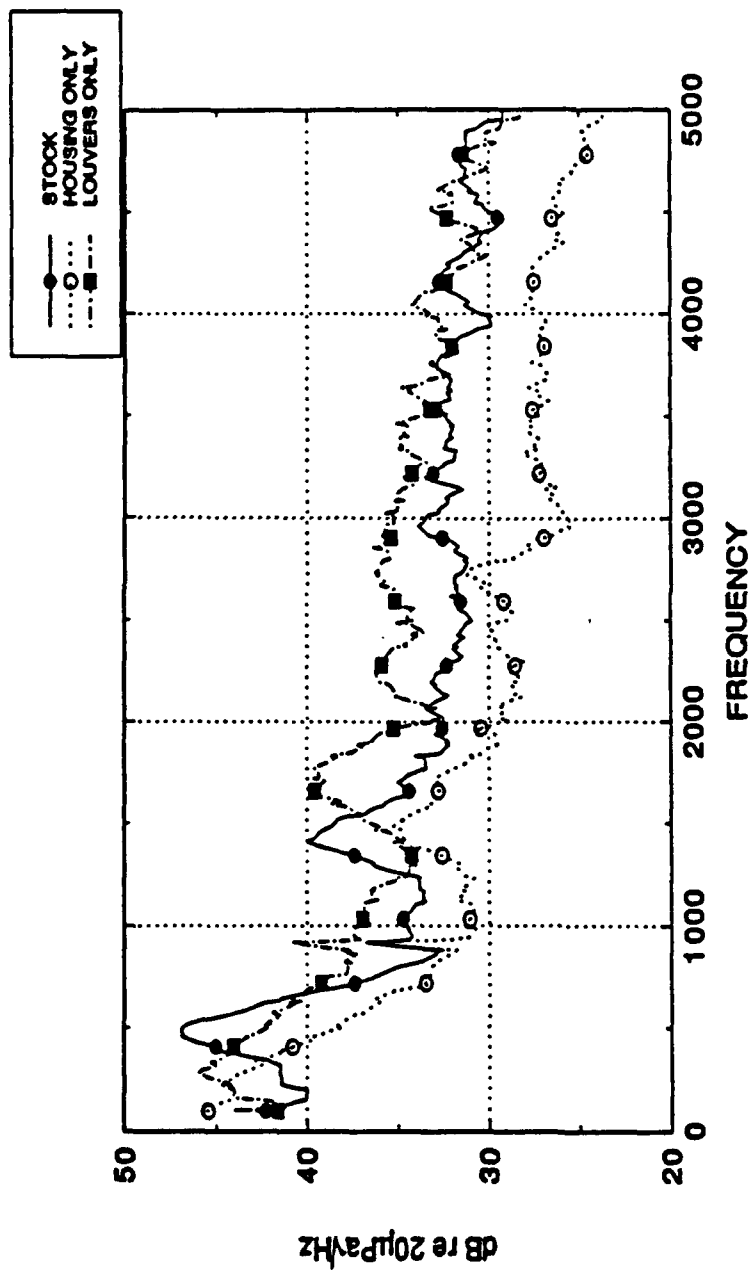
Figure 3.12   PSDs Acquired for Register 3 - Comparison at 5.26 m/s of Stock
Register, Housing only, and Louvers Only.

Figure 3.13   Photograph of Register 5.

31

Separation at BWD Facing Step

Wake

h = 2 mm
L = 13 mm
C = 27 mm

Separation at FWD Facing Step

Laminar
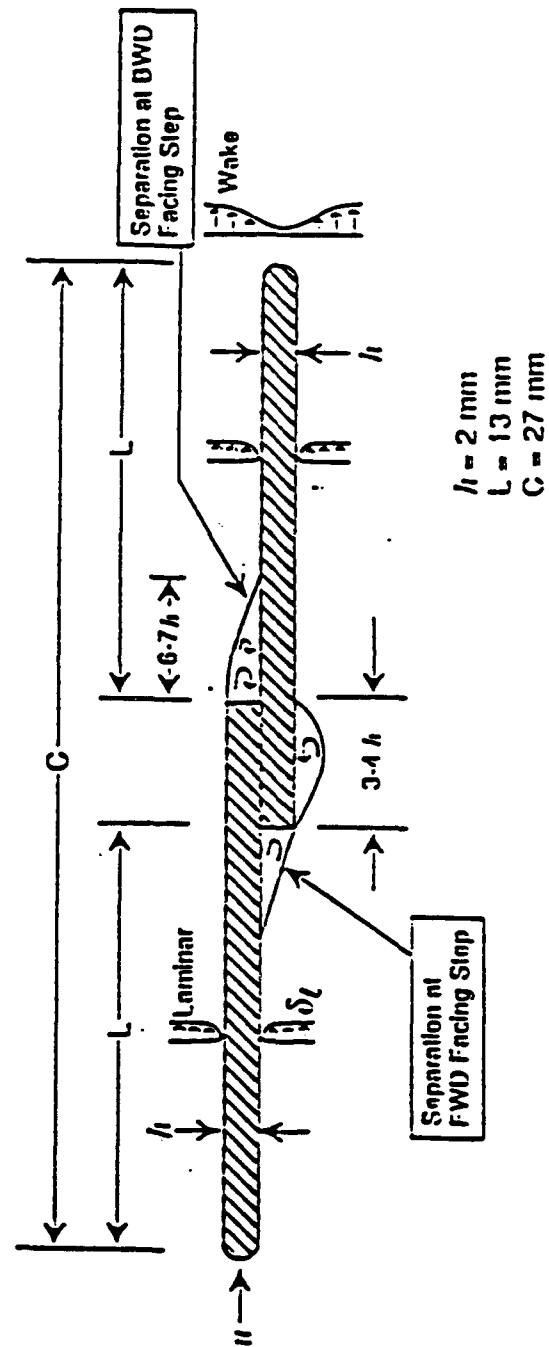
Figure 3.14   Schematic of an Airfoil from Register 5.

The following configurations of this register were evaluated: (1) Stock, (2) Forward step smoothed, (3) Rearward step smoothed, (4) Both steps smoothed, (5) Housing only, (6) Airfoils added one at a time to the housing, (7) Bottom airfoil only, (8) Thumb ridges on bottom airfoil reduced to .5 mm., (9) Thumb ridges on bottom airfoil spaced 3 mm apart.

Power spectra of the radiated acoustic pressure for the stock louver at the seven different velocities are shown in Figure 3.15. These spectra scale with the 6.2 power of velocity. The effect of adding individual airfoils to the register at a free stream velocity of 5.26 m/s is demonstrated in Figure 3.16. A pronounced narrow-band component appears in the 2700 Hz range which is related to the bottom airfoil of the vent. A closer examination of the noise radiated by this bottom airfoil is given in Figure 3.17. The peak observed in Figure 3.16 is seen to be velocity dependent and scales to a Strouhal Number of 0.38 based on the thickness of the trailing edge of the airfoil as shown in Figure 3.18. Increasing the spacing between the thumb ridges by 1 mm decreases the magnitude of the peaks and shifts them to the right as shown in Figure 3.19. As a result, the Strouhal Number shifts to 0.43. Decreasing the height of the ridges by 0.5 mm completely eliminates this peak (Figure 3.20). Thus, the results suggest that the thumb ridges are the cause of the narrow-band acoustic energy. Data for this configuration is available for only the first five velocities.

The rearward and forward facing steps on the individual louver airfoils are responsible for a considerable portion of the high-frequency radiated sound. This is

Figure 3.15   PSDs Acquired for Register 5 - Stock Configuration.
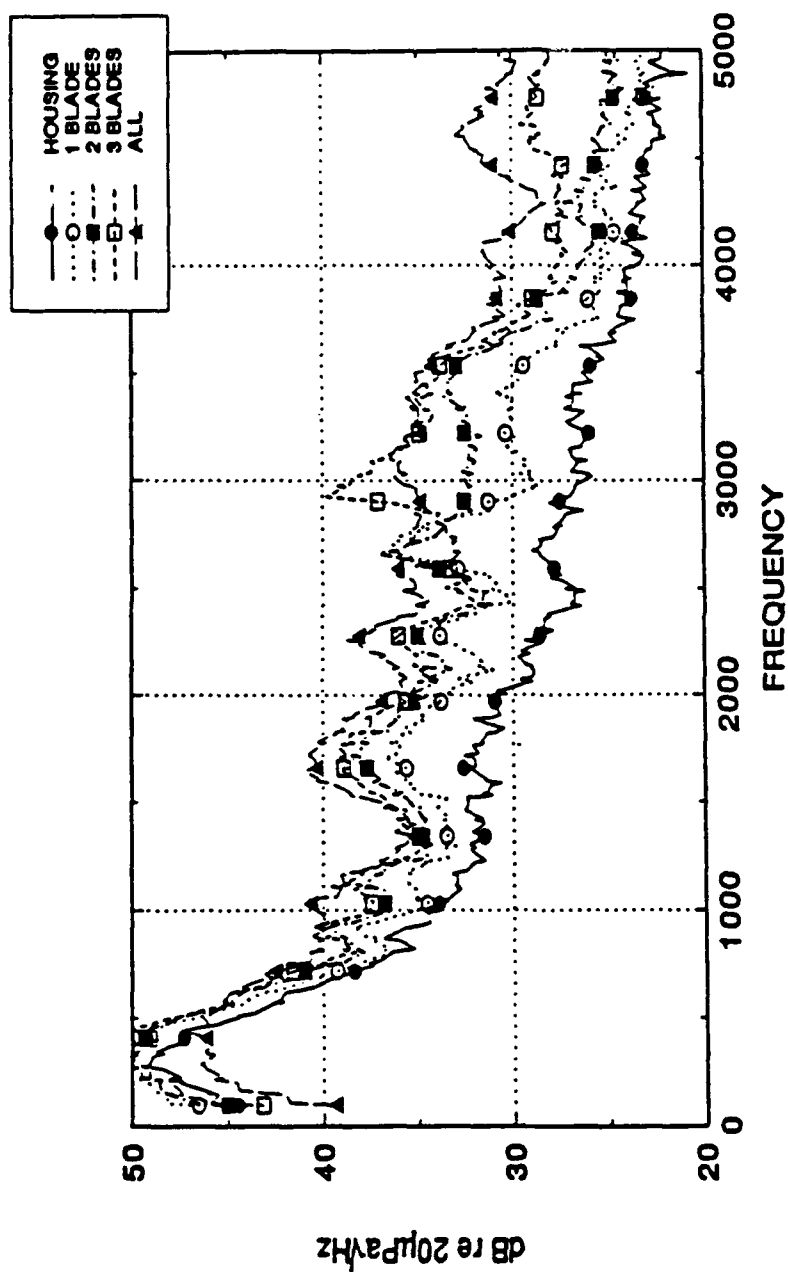
Figure 3.16   PSDs Acquired for Register 5 - Additive Blades.
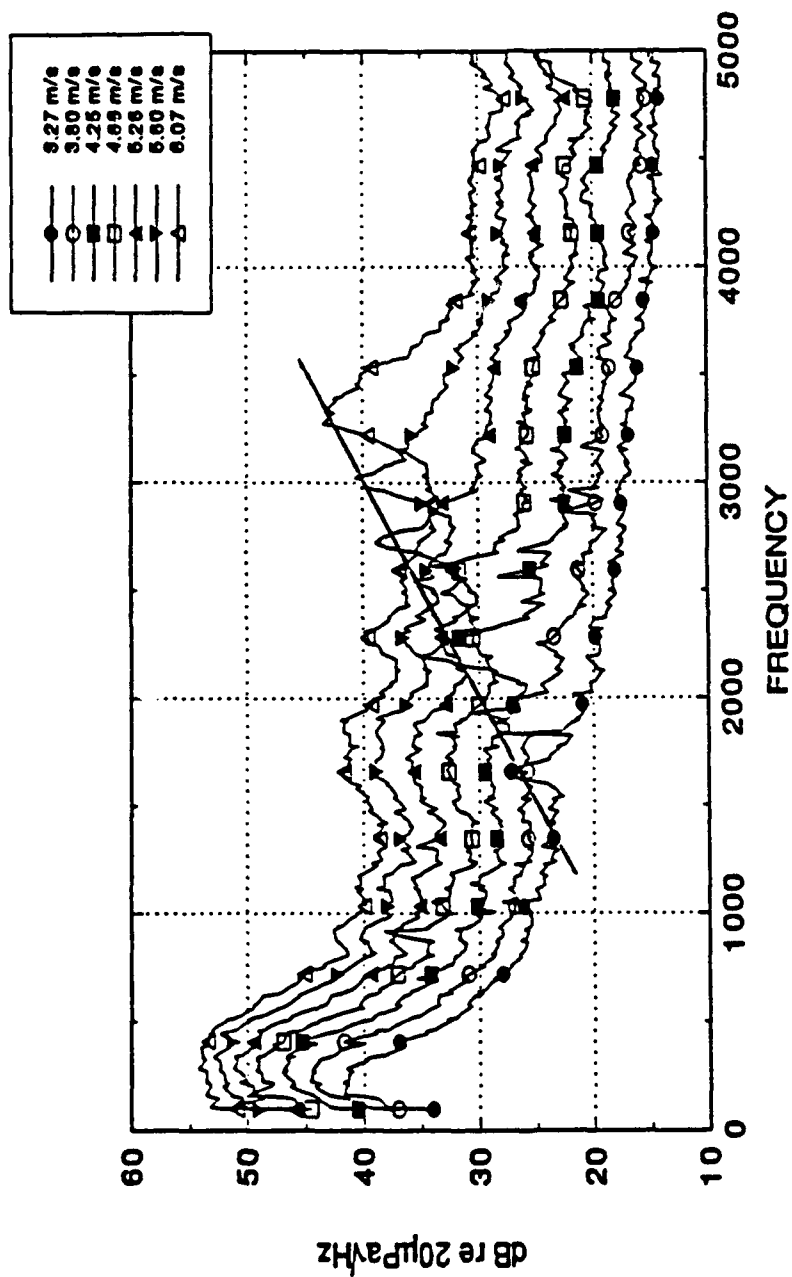
Figure 3.17   PSDs Acquired for Register 5 - Bottom Blade Only.
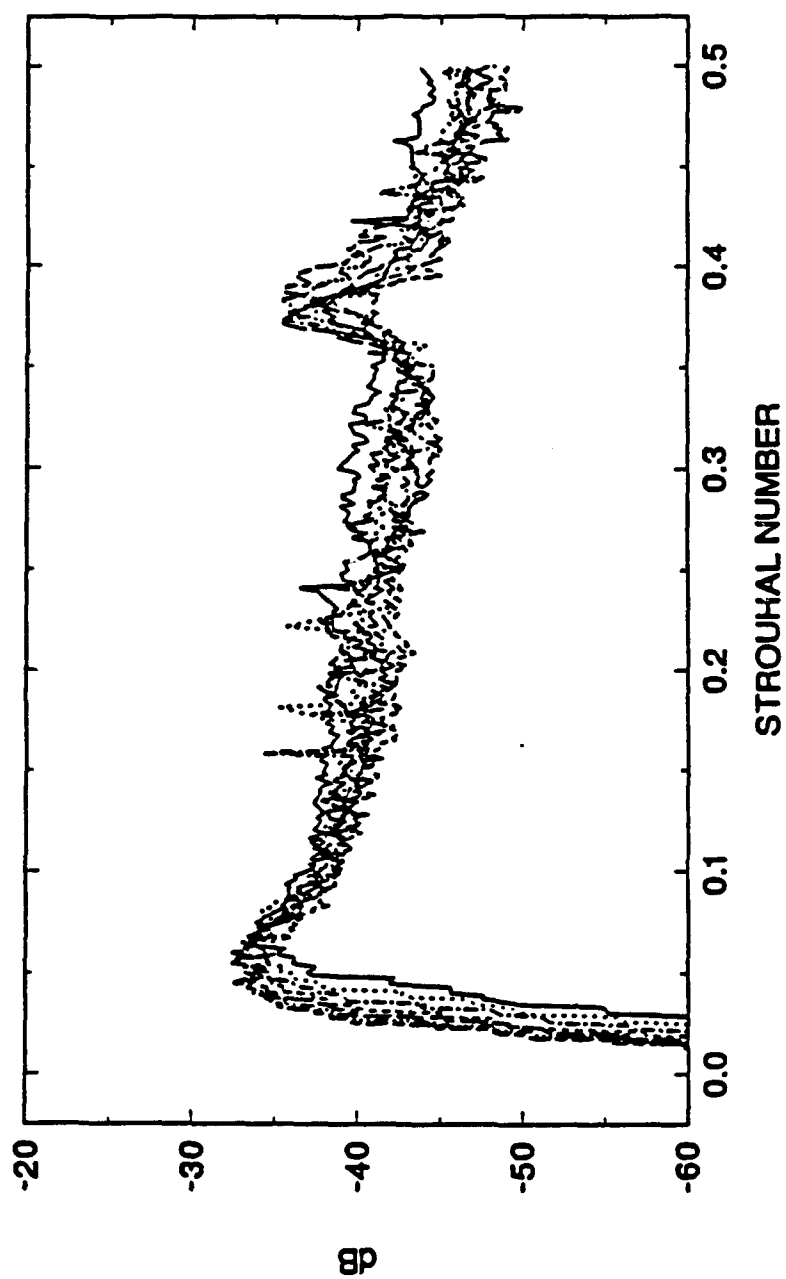
Figure 3.18   *F-Function of Register 5 - Bottom Blade Only.*

37
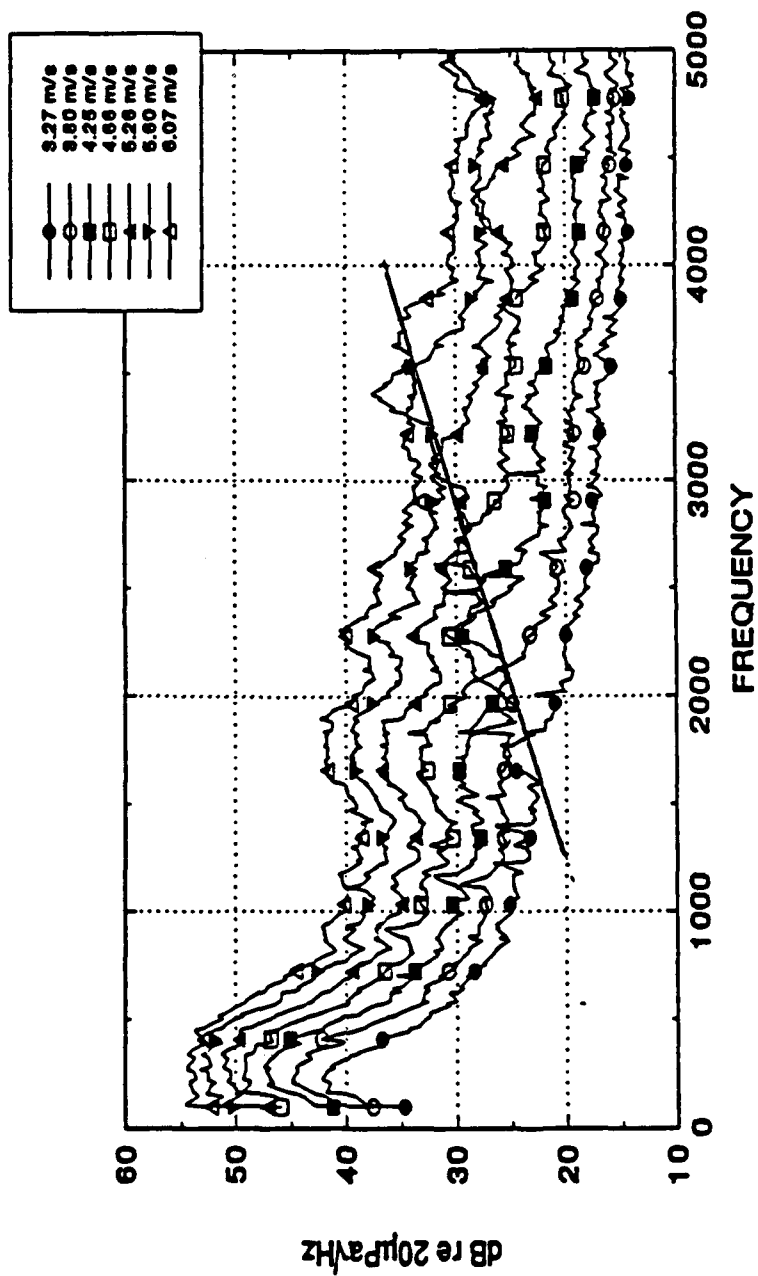
Figure 3.19   PSDs Acquired for Register 5 - Bottom Blade Only Installed
in Register, Every Other Ridge Removed.
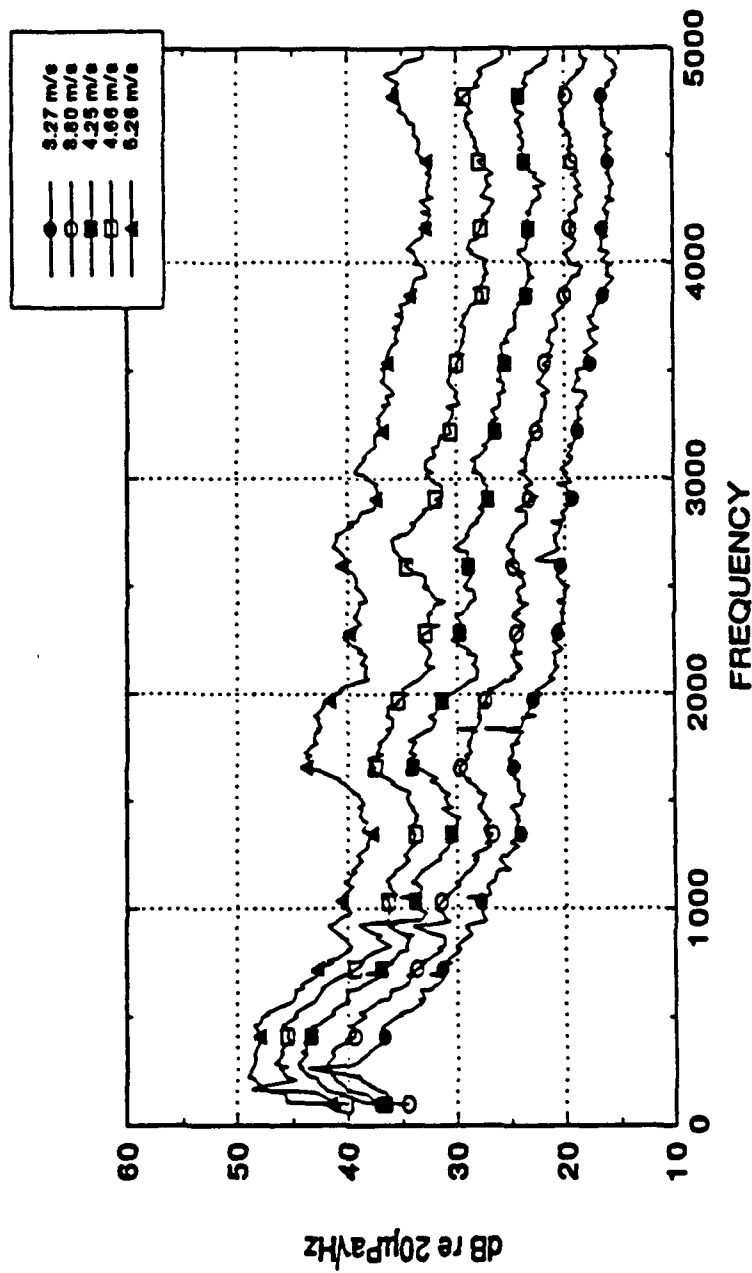
Figure 3.20   PSDs Acquired for Register 5 - Bottom Blade Only,
Ridge Height Reduced to .5 mm.

demonstrated by comparing Figure 3.21 with Figure 3.15, where the data of Figure 3.21 were obtained for a modified register in which the steps were filled in with body putty and sanded smooth. Noise reduction between 3 to 6 dB is achieved above 500 Hz. Further description of this particular register and its aeroacoustics may be found in Reference 9.

3.4 Register 8

Register 8 is a dual airfoil register with six relatively short horizontal airfoils and five long struts. The smaller airfoils are symmetric with a 1 mm thick leading and trailing edge. The longer airfoils have a 2 mm thick leading edge and a 1.5 mm thick trailing edge. Figure 3.22 is a photograph of this register with two of the vertical airfoils removed.

The stock configuration of the register, along with the effect of adding individual airfoils to the housing was evaluated.

Figure 3.23 contains the PSDs of the stock register. No large resonance peaks were observed. A comparison between the noise with housing only and the addition of individual airfoils is shown in Figure 3.24 at an inflow velocity of 5.26 m/s. The addition of one airfoil to the housing caused a 5 dB increase in the 3000 to 4500 Hz range. The addition of a second airfoil caused a 3 dB increase at 2300 Hz. The addition of the third airfoil caused a 3 dB increase from 1500 to 2500 Hz. A very large increase is noticed at 2300 Hz. The forth airfoil caused a 5 dB increase
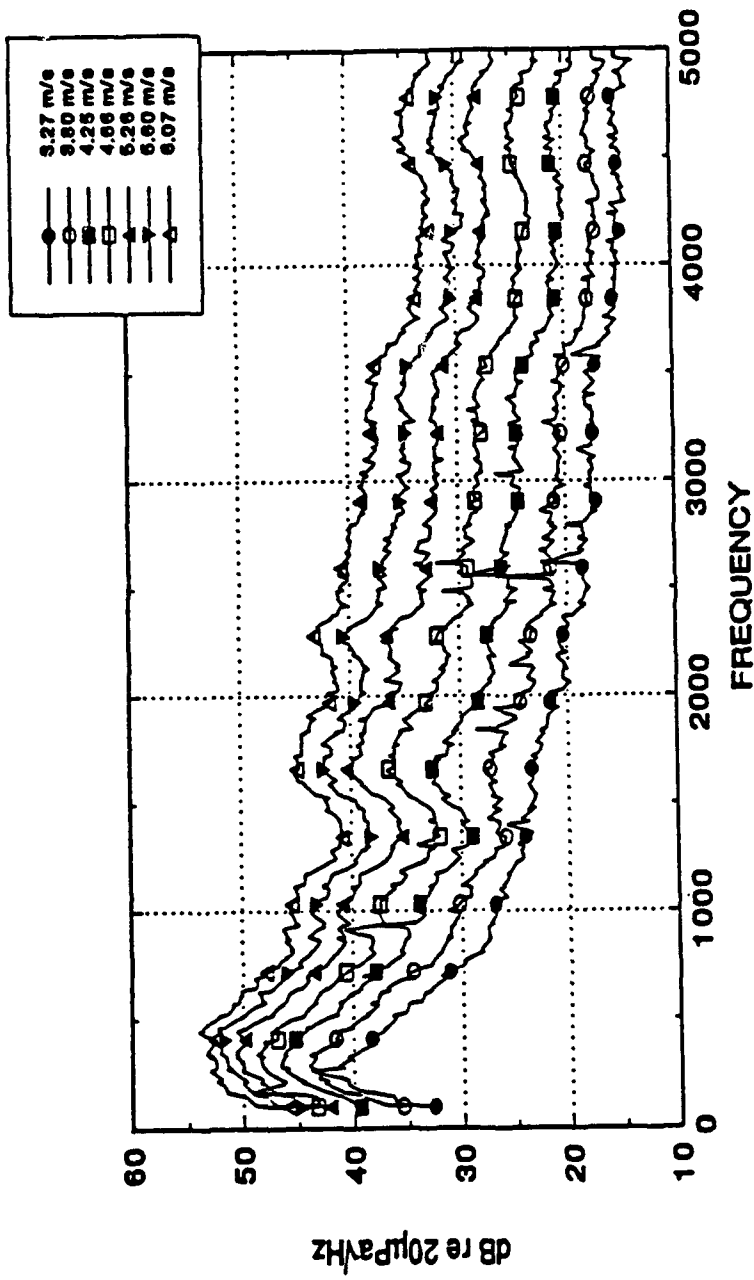
Figure 3.21   PSDs Acquired for Register 5 - Both Steps Filled In (Smooth Airfoil).

Figure 3.22   Photograph of Register 8.
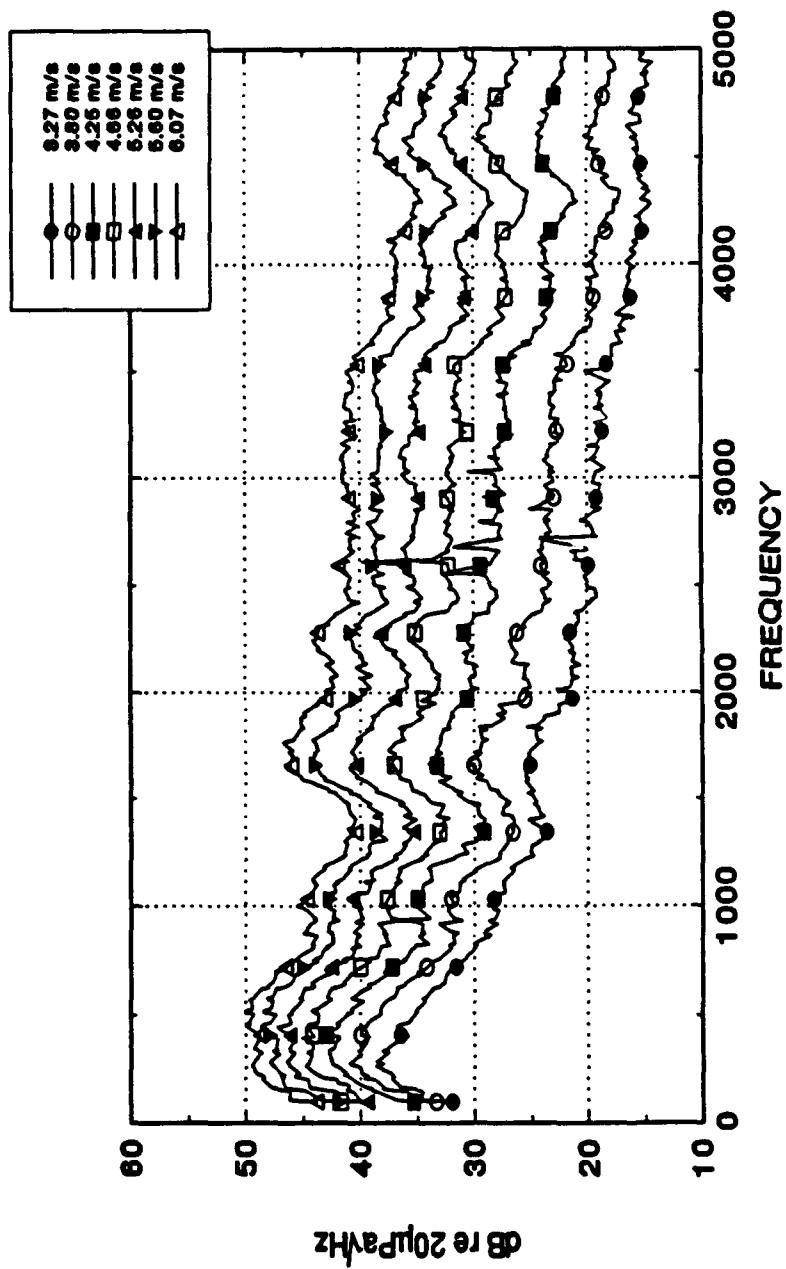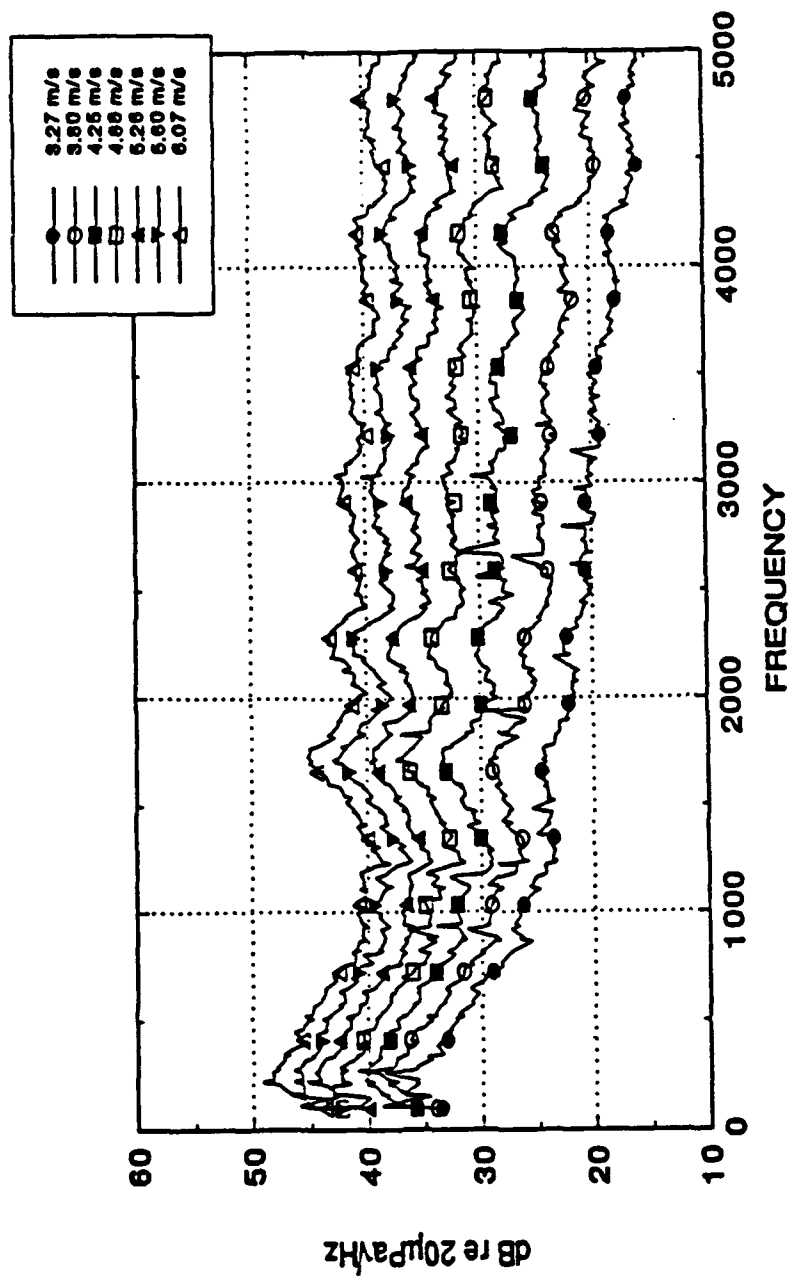
Figure 3.23   PSDs Acquired for Register 8 - Stock Configuration.
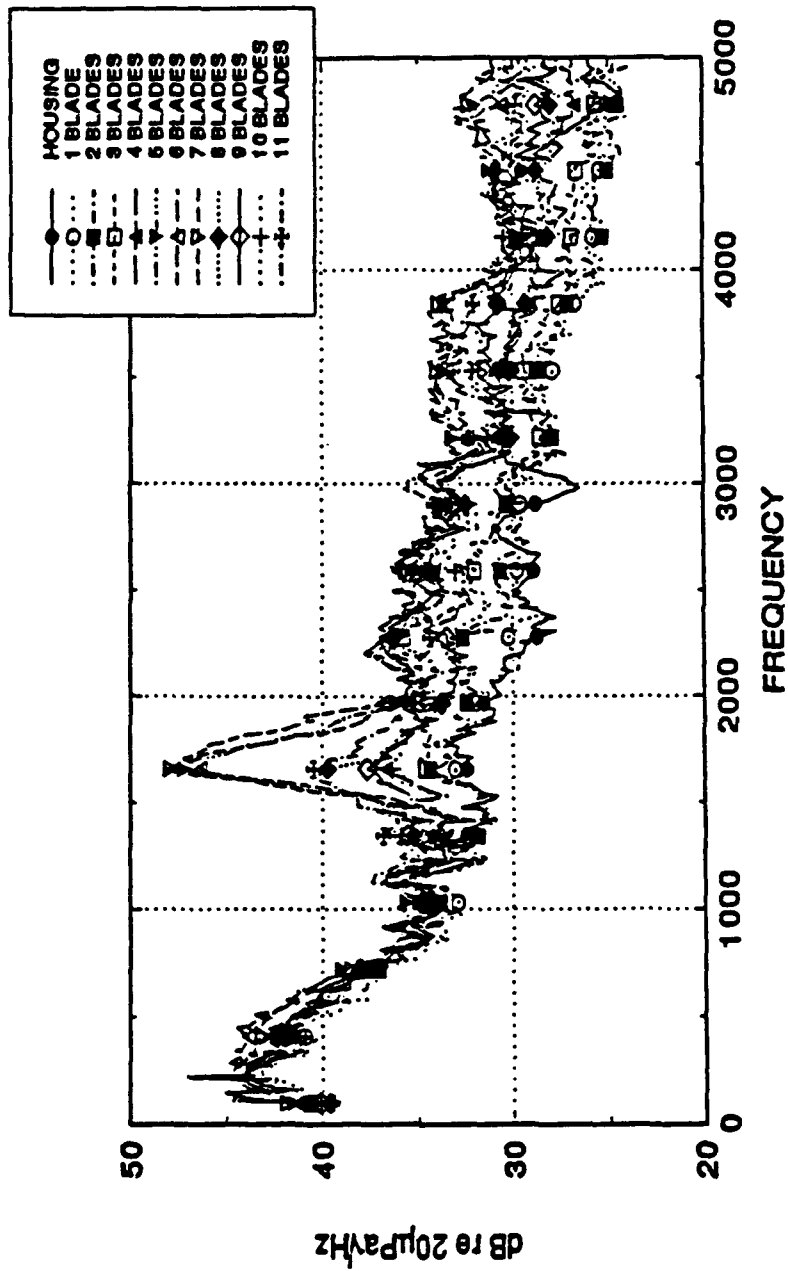
Figure 3.24   PSDs Acquired for Register 8 - Additive Blades.

at 1000, 1600, and 3000 Hz. The addition of the fifth airfoil caused a very large peak to occur at 1600 Hz. This peak is approximately 15 dB higher than the previous spectra. The addition of the 6th airfoil caused no real difference in the noise spectra. The addition of the first vertical airfoil also caused no real difference. The addition of the second vertical airfoil significantly decreased the peak at 1600 Hz. A third vertical airfoil reduced the peak further. This peak became indiscernible once all the airfoils were in place.

Further investigation into the peak at 1600 Hz showed that it is velocity dependent (Figure 3.25). These peaks collapse approximately to a Strouhal Number of .12 based on the trailing edge thickness of the horizontal airfoils (Figure 3.26).

The addition of the airfoils also affects the velocity scaling relationship. The scaling relationship as each airfoil is added along with the effect on the Overall Sound Pressure Level (at 5.26 m/s) is displayed in Table 3.2. It was observed that the OASPL steadily increases with the addition of airfoils until the vertical airfoils were added.

3.5 Register 10

Register 10 is a barrel type of register with seven airfoils and two support struts. It has shut-off door comprised of two plastic pieces with a piece of foam wedged between them. The leading and trailing edges of this register are relatively
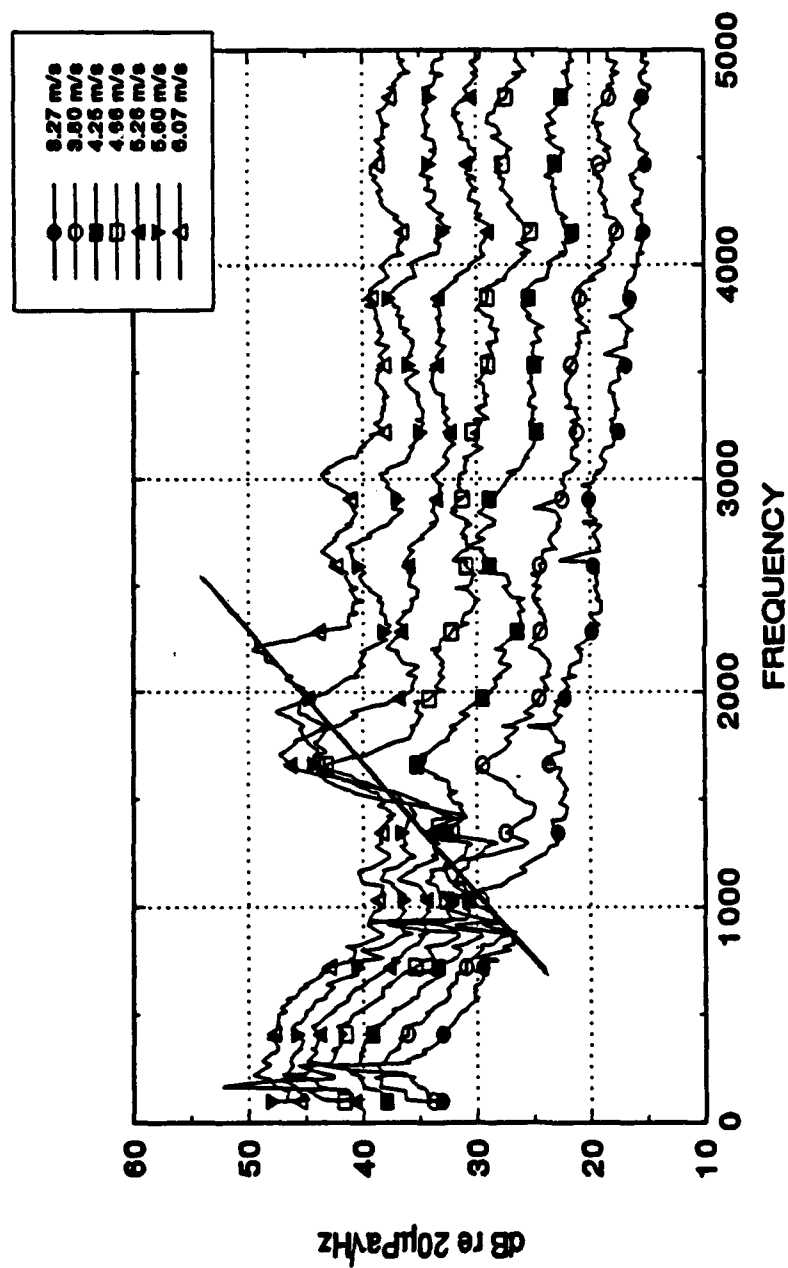
Figure 3.25   PSDs Acquired for Register 8 - 6 Blades Installed in Register.
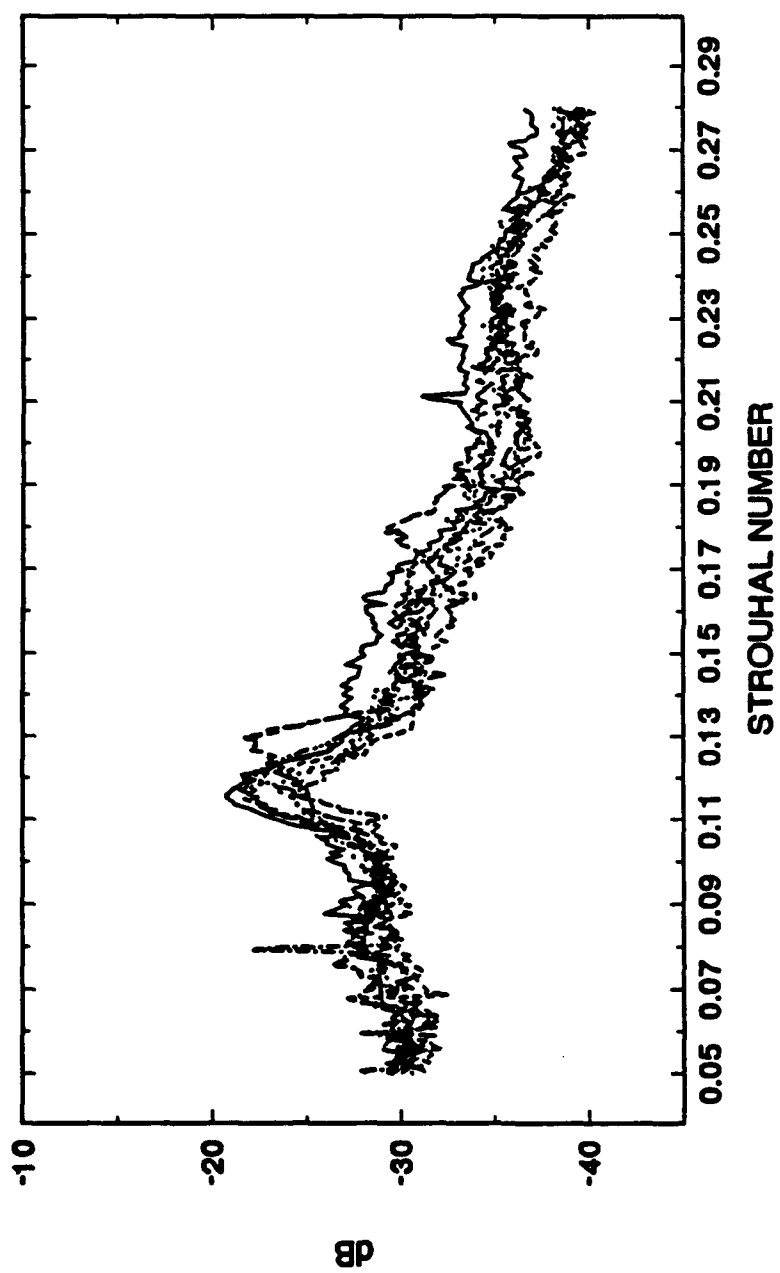
Figure 3.26   F-Function for Register 8 - 6 Blades Installed in Register.

Table 3.2   OASPL and Velocity Scaling for Register 8 - Additive Airfoils

CONFIGURATION	VELOCITY EXPONENT	OASPL
Housing Only	5.4	43.3
1 Airfoil	5.1	44.4
2 Airfoils	5.4	45.0
3 Airfoils	5.7	45.7
4 Airfoils	6.0	46.5
5 Airfoils	6.15	48.8
6 Airfoils	6.30	49.0
7 Airfoils (First Vertical Airfoil)	6.12	48.9
8 Airfoils	6.45	46.5
9 Airfoils	6.07	46.5
10 Airfoils	5.7	46.1
11 Airfoils (All Airfoils in Place)	6.3	47.0

thick compared to the others. The airfoils have a 2 mm trailing edge and a 3 mm leading edge. The support struts are 3 mm thick. Figure 3.27 is a photograph of the register.

Three configurations were evaluated: (1) Stock, (2) Stock - shut-off door cavity filled in, and (3) Stock - without the shut-off door.

Figure 3.28 contains the spectra acquired of the stock register. The spectra scale to the 5.9 power of velocity. The influence of the shut-off door cavity on the radiated noise was small as shown in Figure 3.29. The removal of the shut-off door caused a 3 dB decrease in the noise levels from approximately 1400 to 1600 Hz.

3.6 Register 20

Register 20 is a square barrel type of register with three airfoils and three support struts. The shut-off door is square with a piece of foam between the plastic pieces. The airfoils have thick, rounded leading and trailing edges. The support airfoils are 2 mm thick. Figure 3.30 is a photograph of this register.

Two configurations of this register were evaluated: (1) Stock, (2) Stock without the shut-off door.
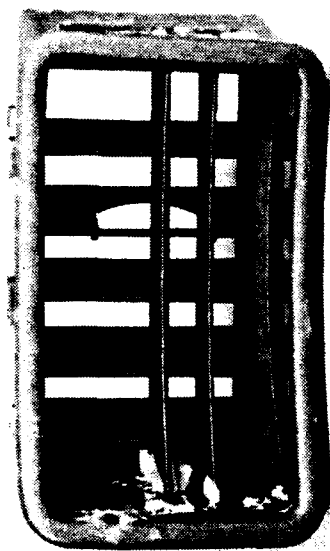
Figure 3.27   Photograph of Register 10.
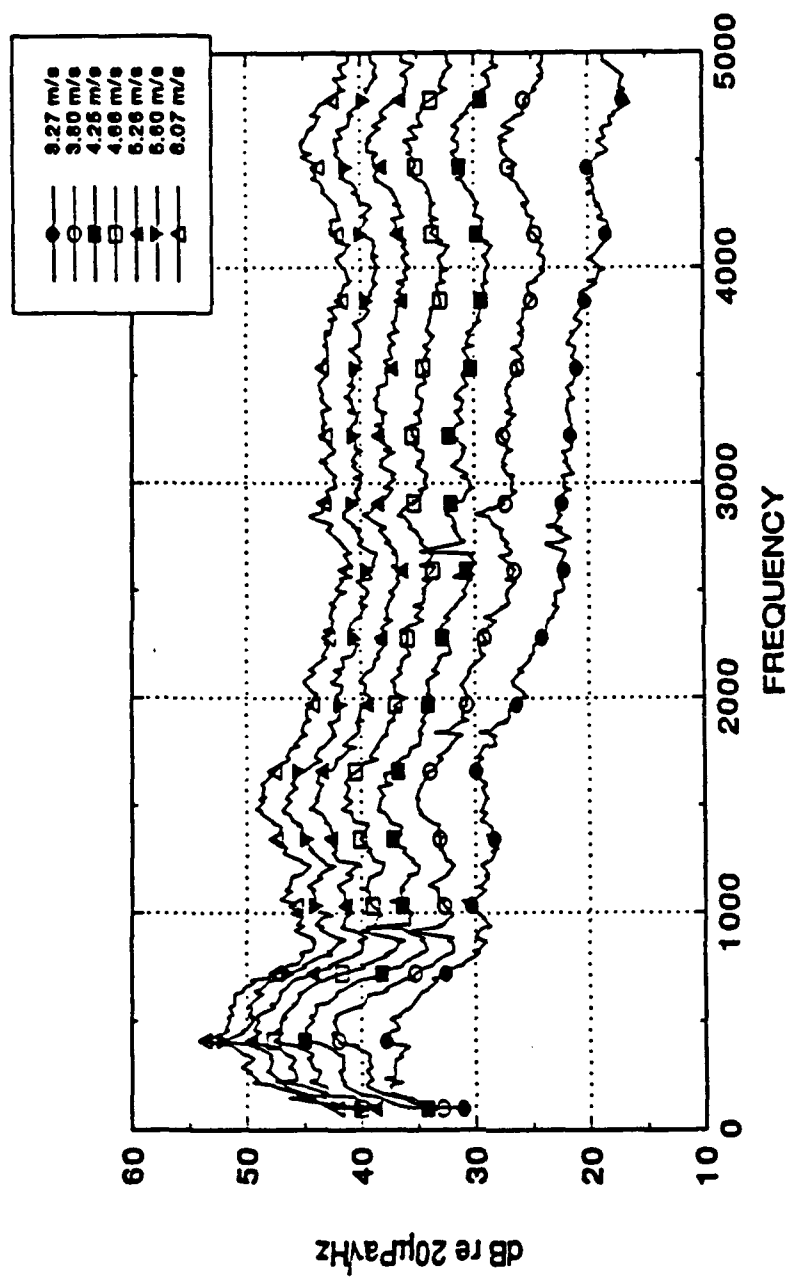
Figure 3.28   PSDs Acquired for Register 10 - Stock Configuration.
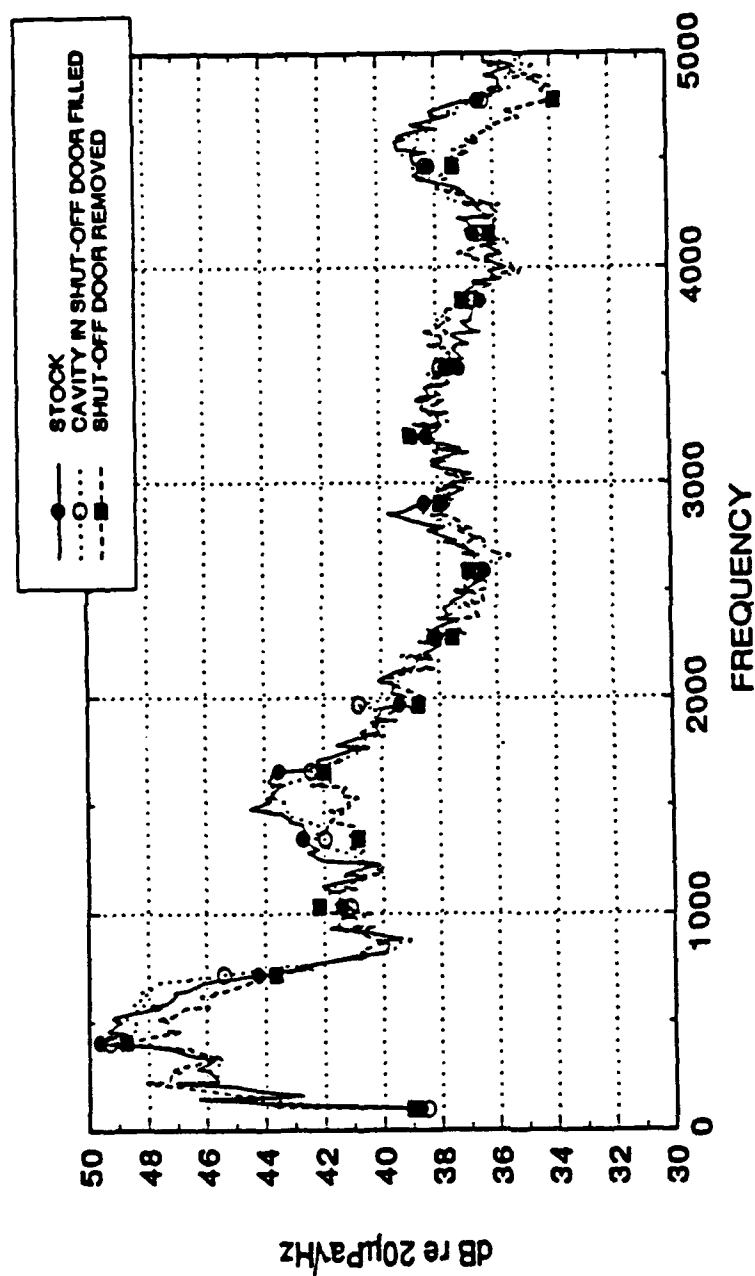
Figure 3.29   PSDs Acquired for Register 10 - Stock, Stock with Shut-off Door Cavity Filled, and Stock Without Shut-off Door at 5.26 m/s.
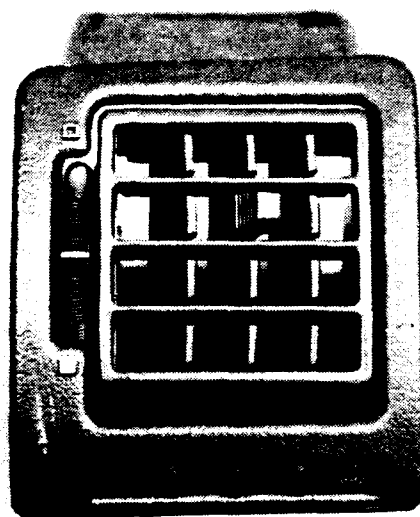
Figure 3.30   Photograph of Register 20.

Figure 3.31 are the PSDs collected for the stock configuration of register number 20. The spectra scale to the 6.2 power of velocity. A definite velocity dependent peak is noticed below 1000 Hz. This peak is not evident when the shut-off door is removed (Figure 3.32), so it is related to the presence of the shut-off door. These peaks collapse to a Strouhal Number of 0.20 using the thickness of the door as the length scale. Figure 3.33 is the F(St) Function calculated for the stock configuration of this register.

3.7 Unmodified Registers

Register 7 is a dual vane type register. This register has a very small inlet area and an angled duct which forces the airflow to impede the louvers at a $45°$ angle. Figure 3.34 is a photograph of this register.

The PSDs acquired for register number 7 are presented in Figure 3.35. The power spectra scale to the 6.6 power of velocity. A low frequency velocity dependent peak is observed, which scales to a Strouhal Number of 0.25 using the trailing edge thickness of the forward airfoil (3 mm) for the length scale.
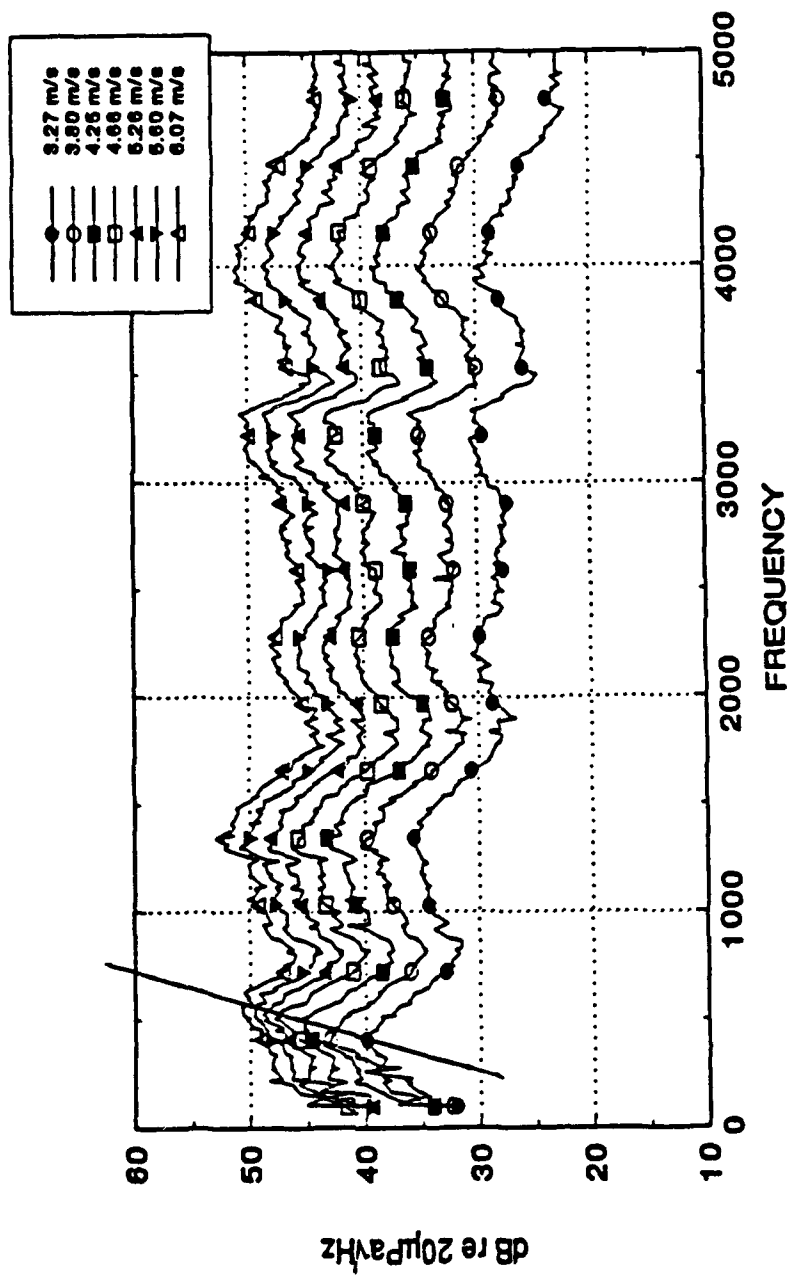
Figure 3.31   PSDs Acquired for Register 20 - Stock Configuration.
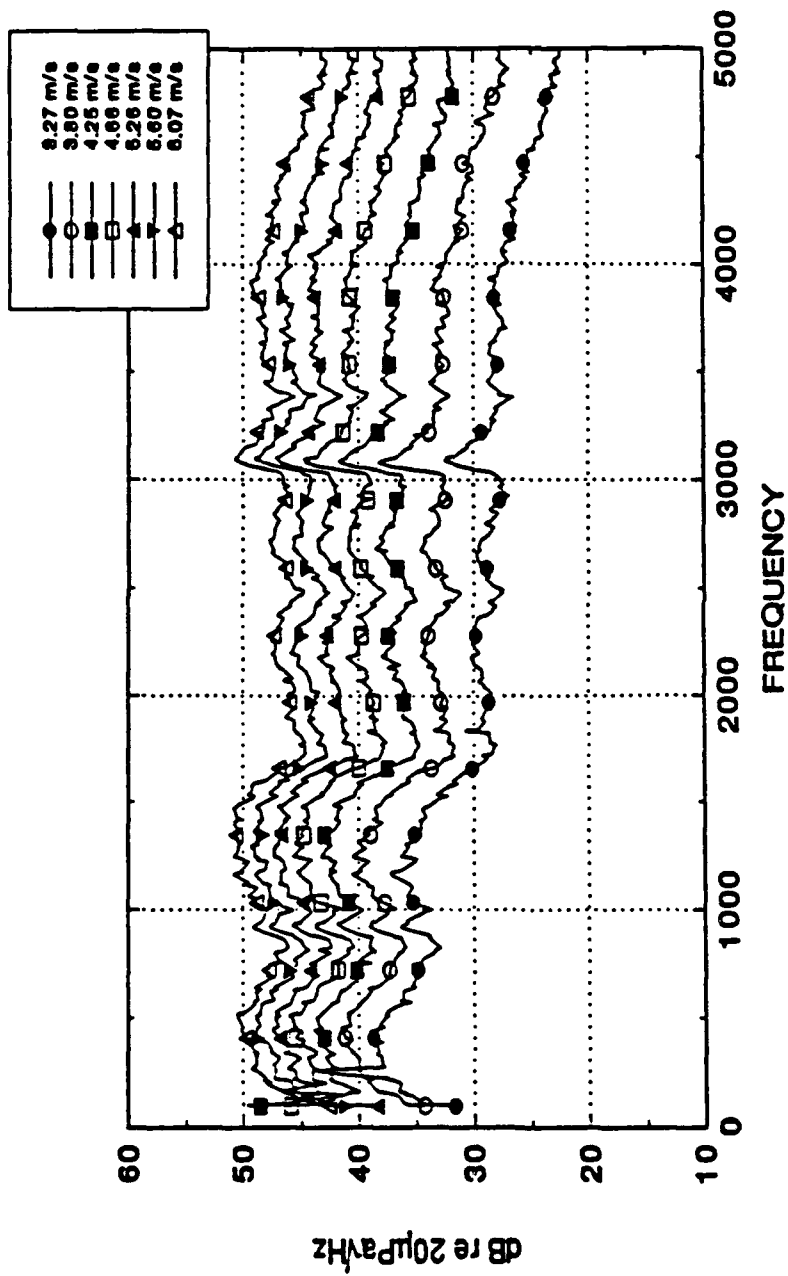
Figure 3.32   PSDs Acquired for Register 20 - Shut-off Door Removed.
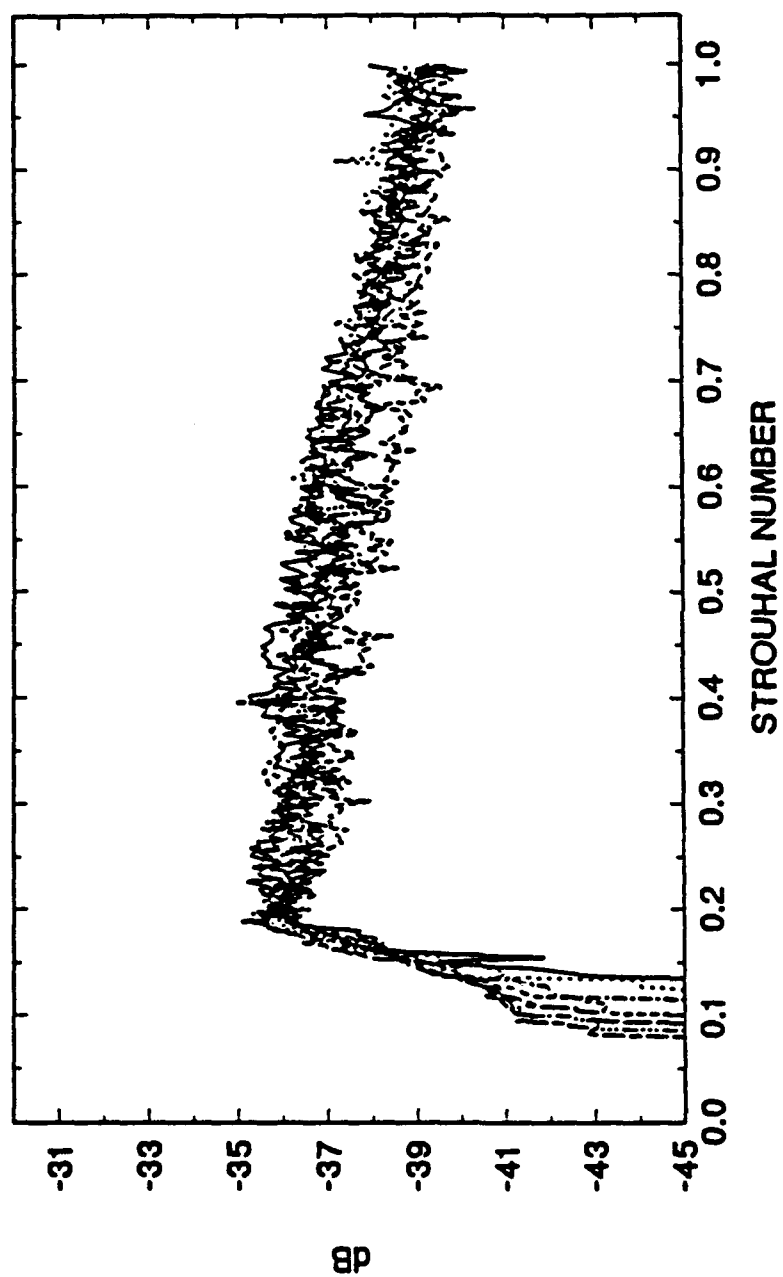
Figure 3.33   F-Function of Register 20 - Stock Configuration.
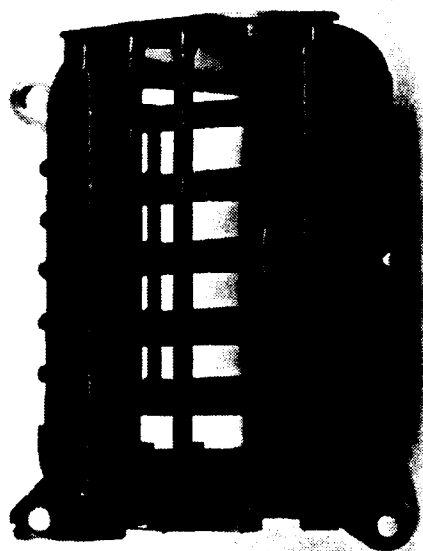
Figure 3.34   Photograph of Register 7

58
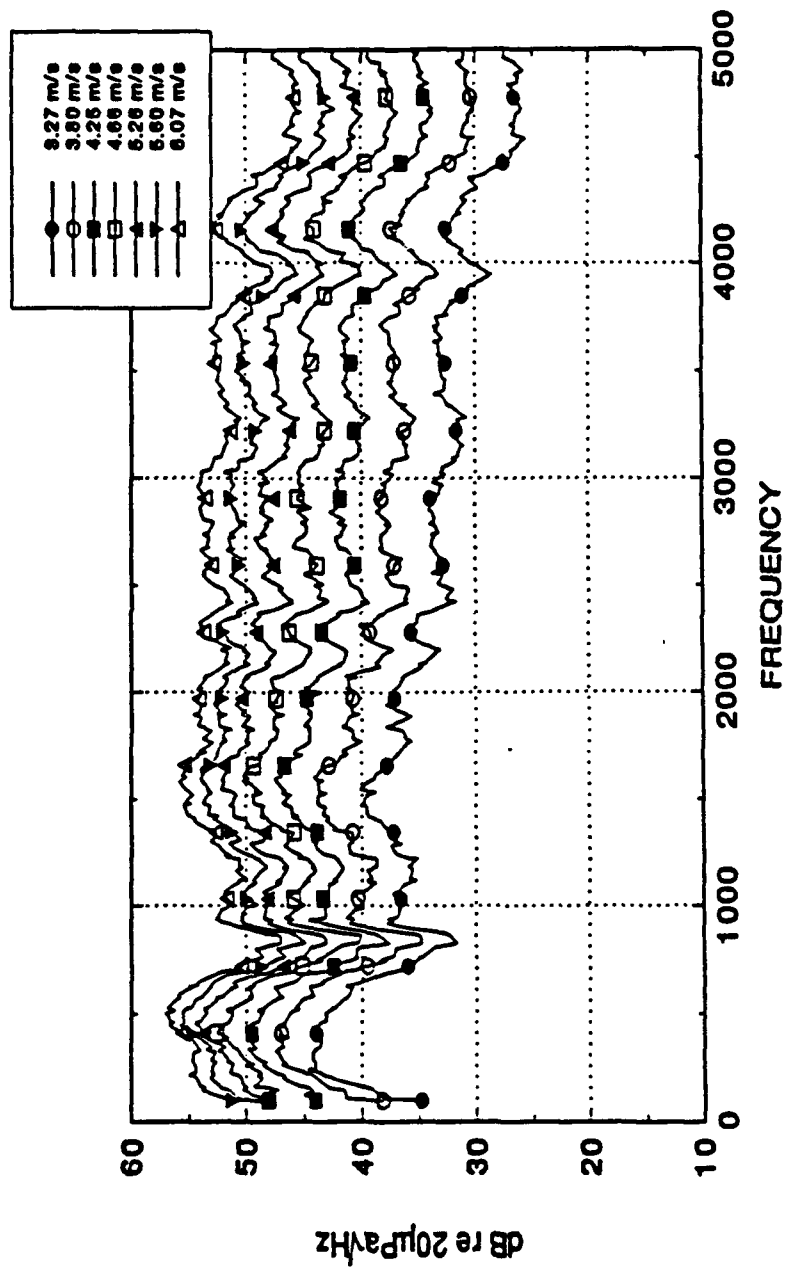
Figure 3.35 PSDs Acquired for Register 7 - Stock Configuration.

Register 9 is a dual vane register. The leading and trailing edges of both sets of airfoils are blunt. Figure 3.36 is a photograph of this register. Figure 3.37 contains the PSDs for the seven test velocities. The power spectra scale to the 6.0 power of velocity.

Register 14 is a barrel type of register with three airfoils and six immovable struts. The leading and trailing edges of this register are rounded and thick. No photograph is available for this register. Figure 3.38 contains the spectra acquired for the stock register 14. These power spectra scale to the 6.0 power of velocity. A strong band of energy is noticed to exist around 1800 Hz.

Register 15 is a small barrel type of register with five airfoils and no struts. A photograph of this register is shown in Figure 3.39. Figure 3.40 are the PSDs acquired for this register. A very definite resonance peak is apparent at 1800 Hz. This peak becomes more prevalent as the velocity is increased. These broadband power spectra scale to the 5.8 power of velocity.

Register 16 is a barrel type of register with ten airfoils and two support struts. The airfoils have a thick rounded leading edge and a blunt trailing edge. Figure 3.41 is a photograph of this register. Figure 3.42 shows the PSDs collected for register number 16. A moderately strong band of energy, independent of velocity, is observed at 2400 Hz and 3600 Hz. The power spectra scale to the 5.6 power of velocity.

Register 17 is a barrel type of register with three airfoils and two small support struts. The airfoils have a blunt leading edge and a very sharp trailing edge.
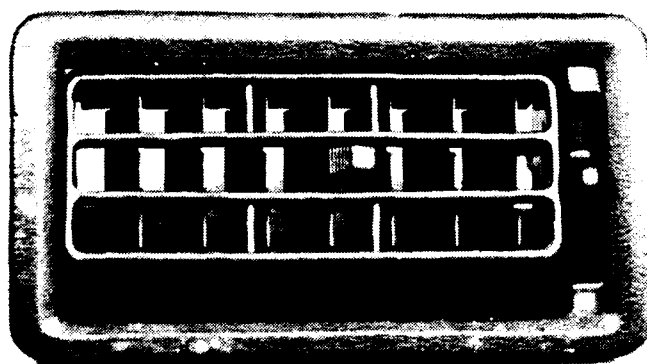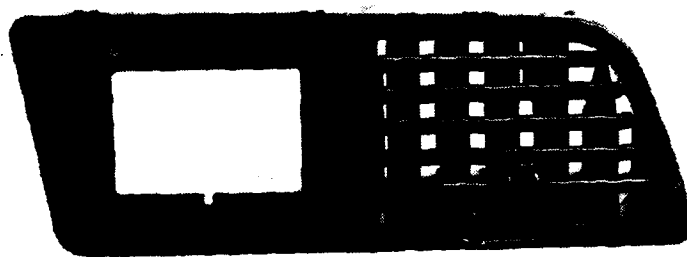
Figure 3.36   Photograph of Register 9.
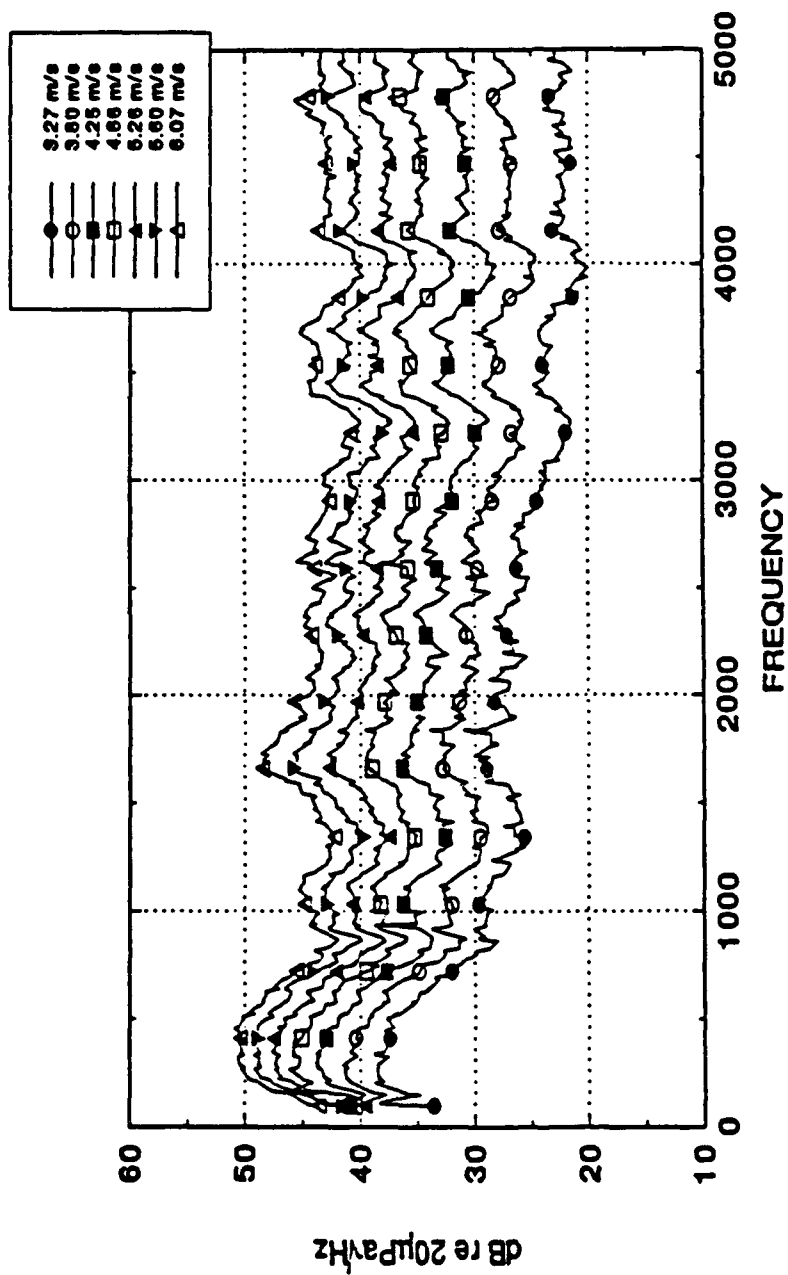
Figure 3.37   PSDs Acquired for Register 9 - Stock Configuration.
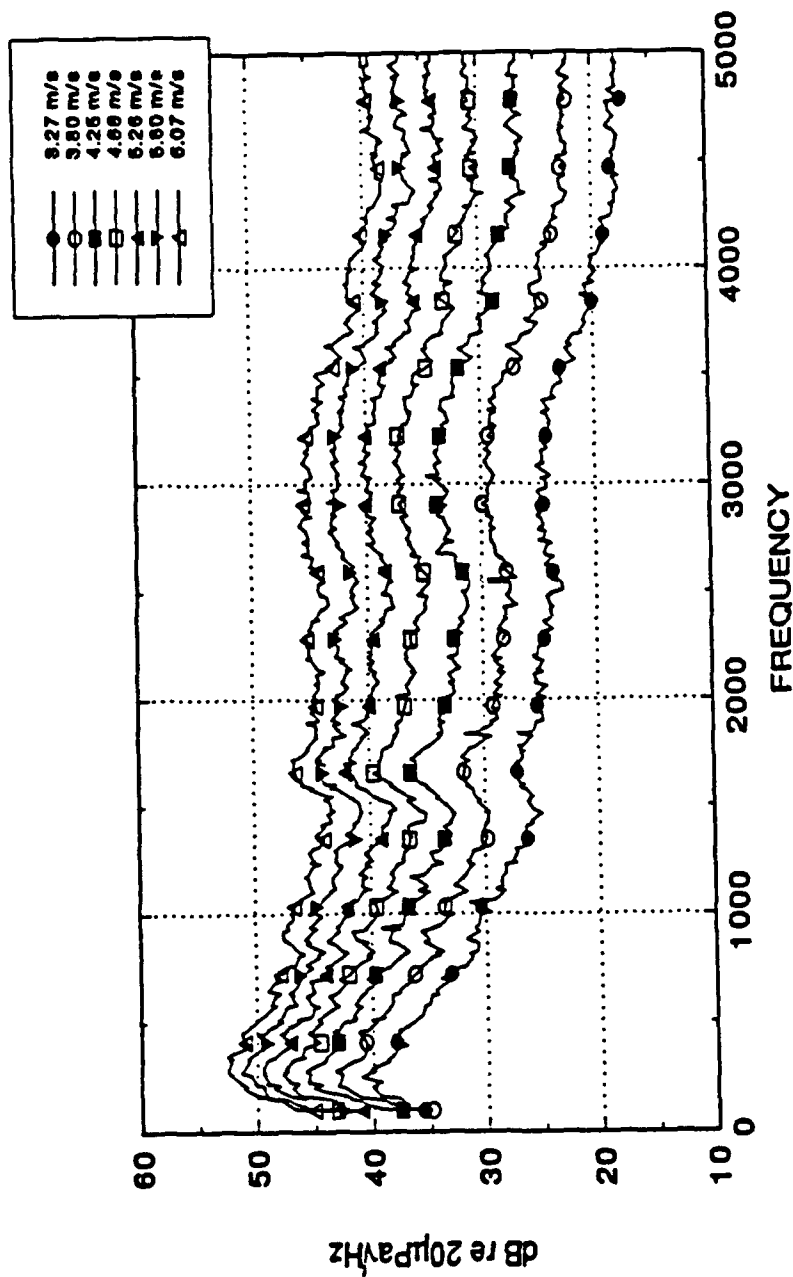
Figure 3.38   PSDs acquired for Register 14 - Stock Configuration.
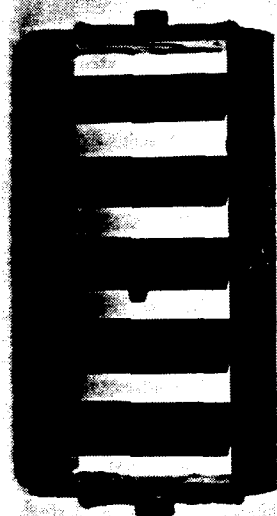
Figure 3.39   Photograph of Register 15.
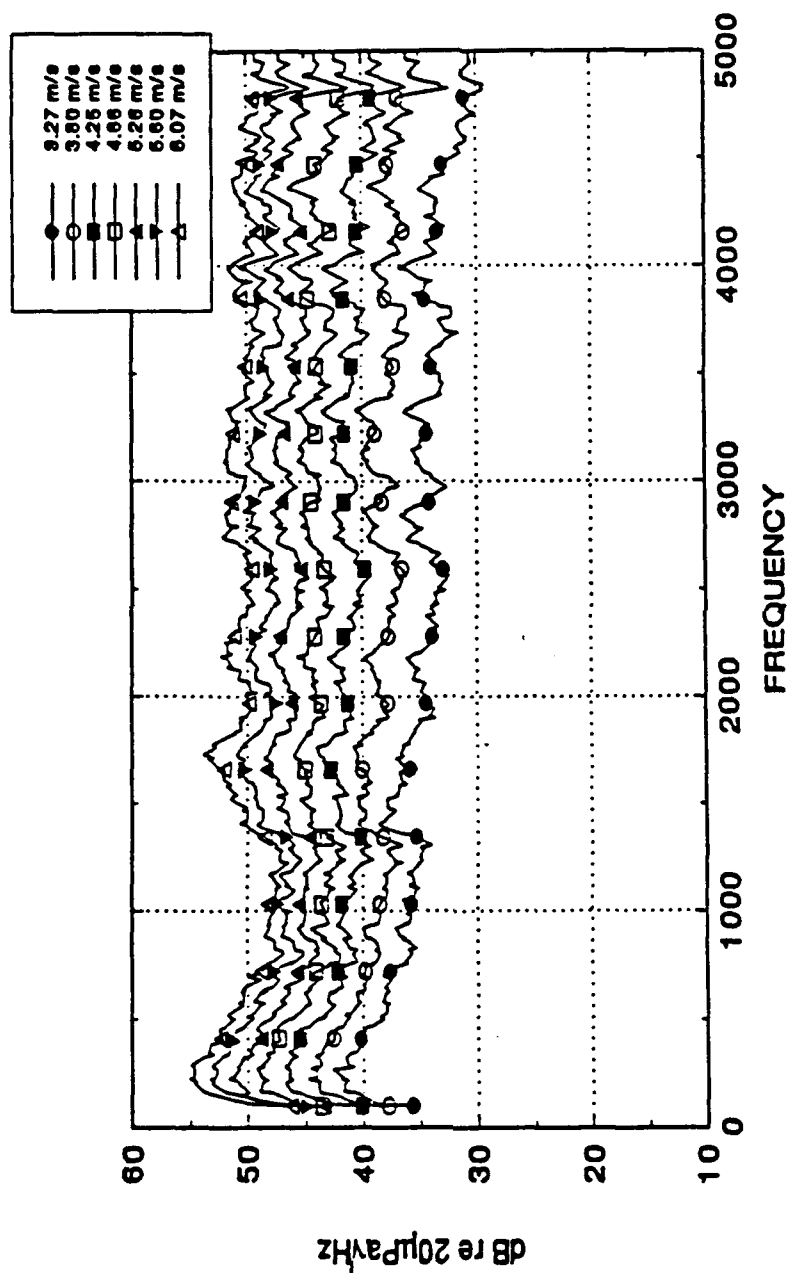
Figure 3.40   PSDs Acquired for Register 15 - Stock Configuration.
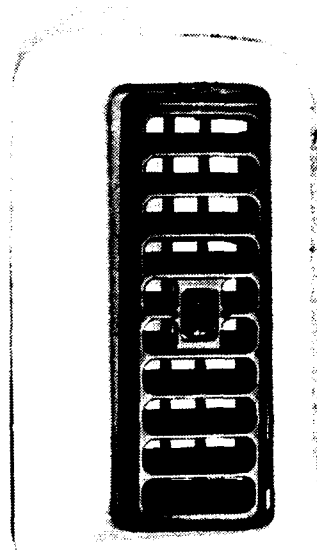
Figure 3.41 Photograph of Register 16.
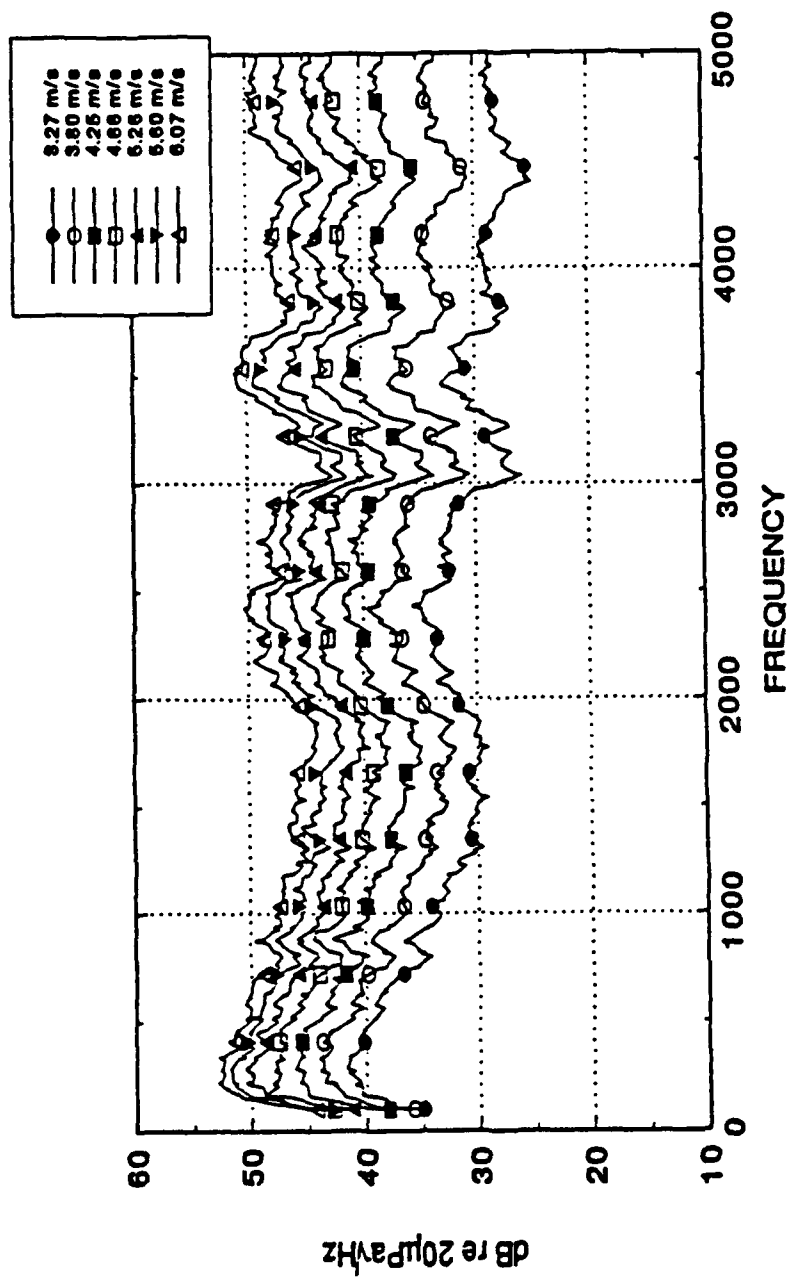
Figure 3.42   PSDs Acquired for Register 16 - Stock Configuration.

A photograph is presented in Figure 3.43. Figure 3.44 contains the PSDs collected for register number 17. The spectra are broadband in nature and scale to the 5.7 power of velocity.

Register 30 is a small barrel type of register with five airfoils and no support struts (Figure 3.45). The airfoils are symmetric with rounded leading and trailing edges 1 mm thick. Figure 3.46 shows the PSDs collected for register 30. The spectra scale to the 5.5 power of velocity. A velocity-dependent peak is observed for the lower three velocities in the 2000 to 3000 Hz range, after which the broadband noise of the louvers masks the peak. These peaks collapse to a Strouhal Number of 0.24 based on a length scale of 1 mm which is the airfoil thickness at the trailing edge.
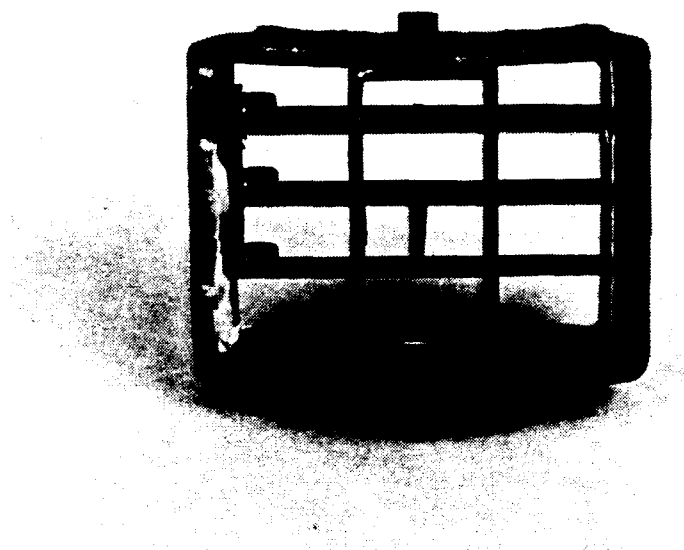
Figure 3.43   Photograph of Register 17.
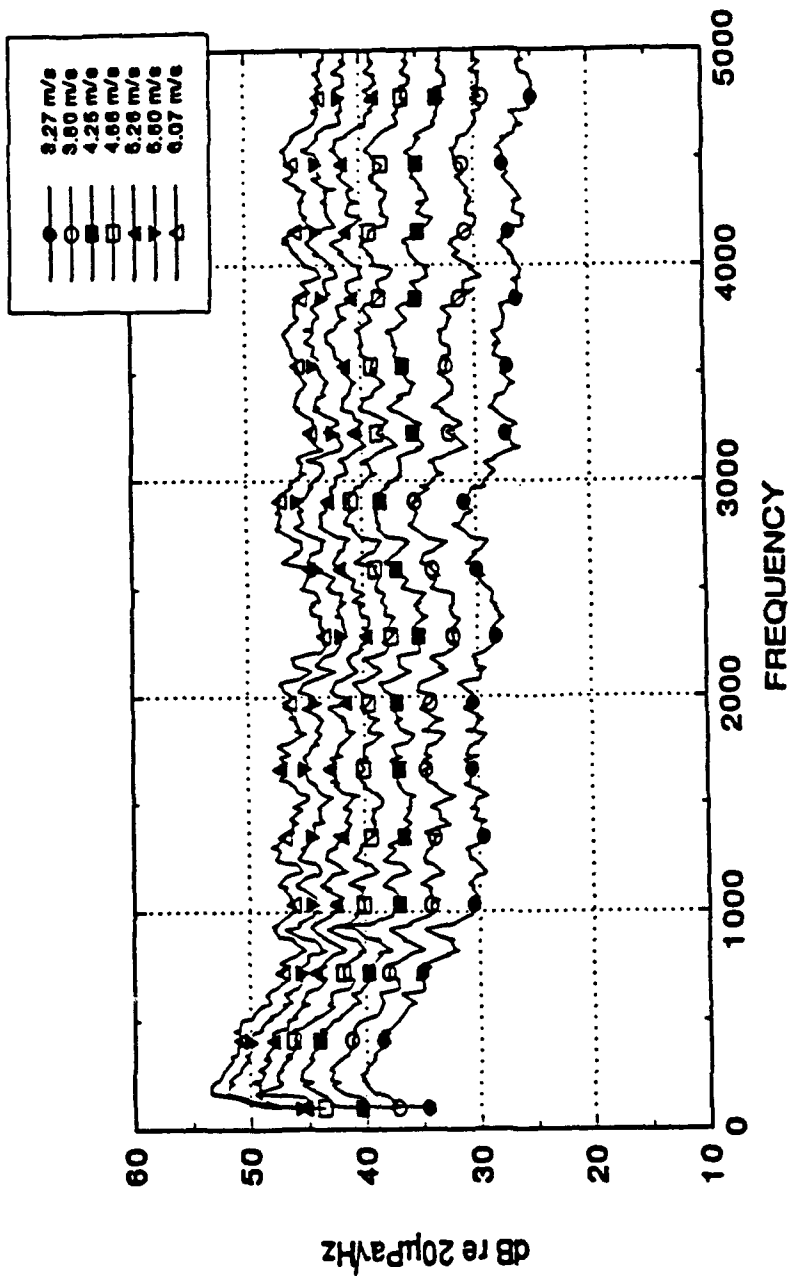
Figure 3.44   PSDs Acquired for Register 17 - Stock Configuration.

Figure 3.45   Photograph of Register 30.
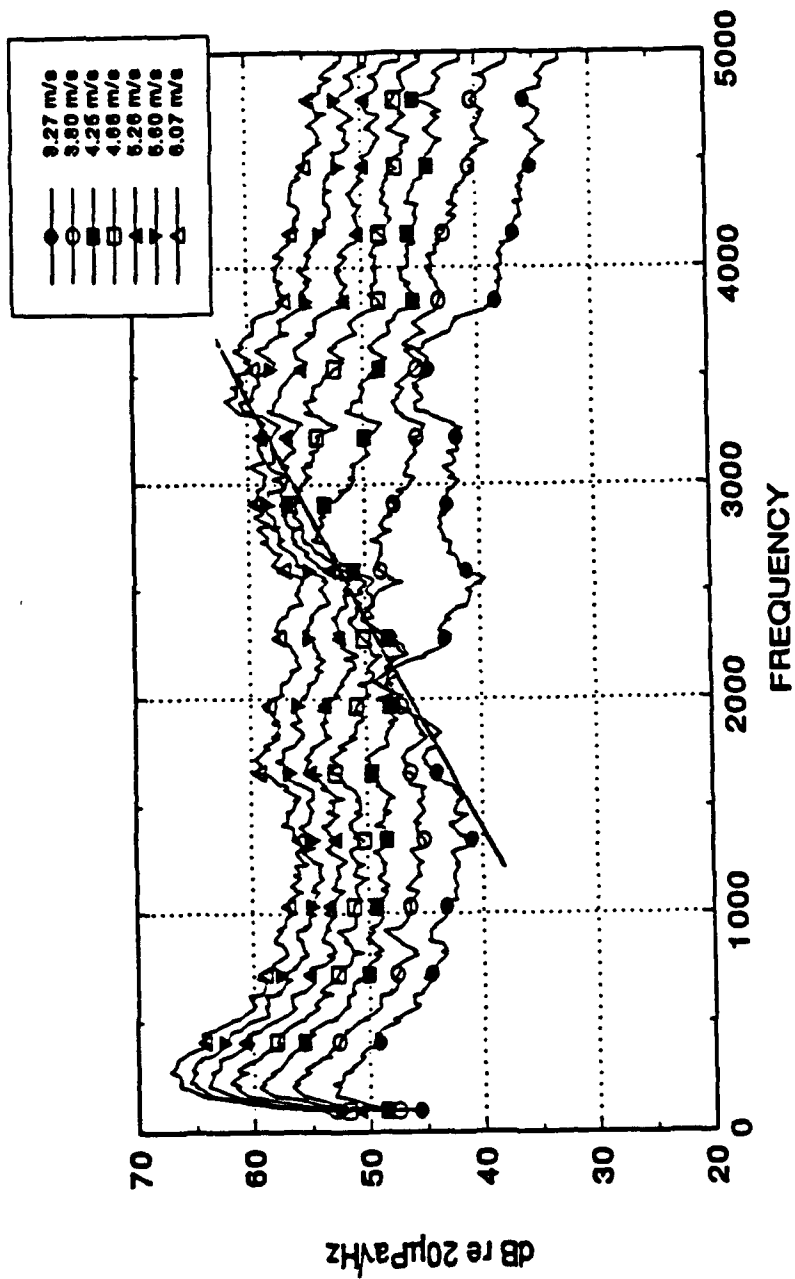
Figure 3.46   PSDs Acquired for Register 30 - Stock Configuration.

Chapter 4

ANALYSIS OF EXPERIMENTAL RESULTS

In this chapter we will analyze the solidity effects, velocity scaling dependence, and other physical parameters on the acoustic signature radiated by the registers.

The longest chord on any of the registers is 37 mm (Register 1); therefore, the maximum Reynolds Number achievable is 15,113. This is smaller than the critical value of $2x10^5$, and it is therefore assumed that the boundary layer at the trailing edge region of each of the configurations tested is laminar.

4.1 Velocity Scaling

On the average, the spectra of the stock registers scaled to the 6th power of velocity (based on overall levels). This is indicative of a dipole source, as is to be expected from airfoil theory. This scaling law persisted regardless of the number of airfoils and other physical obstructions present in the register.

4.2 Strouhal and Geometry Dependence

Figure 4.1 is a comparison of the measured overall sound pressure level (OASPL) for each register at an inflow velocity of 4.66 m/s. Register 7 has a high level due to the inherent non-zero angle of attack of the flow on the vanes and a small inlet area. Register 8 had the lowest level due to its large inlet and outlet area.

Figure 4.2 depicts the dependence of OASPL on the total inlet area of each register. Figure 4.3 presents the dependence of OASPL on the outlet area. Figure 4.4 presents OASPL as a function of the ratio between the inlet and outlet area. The OASPL tends to increase as the outlet area decreases with respect to inlet area.

Figure 4.5 shows the effect of adding individual blades to the housings of register 5 and register 8. The initial increase in the OASPL with the number of blades, N, are the same for each register, indicating an N-dependence on OASPL exists. Thus, for $N \leq 4$, OASPL scales on $N^{2/5}$. The higher OASPL of Register 5 can be attributed to a smaller air inlet area. The linear increase in OASPL is interrupted when the fifth horizontal airfoil was added to register 8. The large increase in sound pressure level is due to a Strouhal effect. This effect is eliminated when the vertical struts were added to the register. The struts are likely to decorrelate the local pressure fluctuations along the trailing edge, which reduces the intensity of trailing edge sound production.
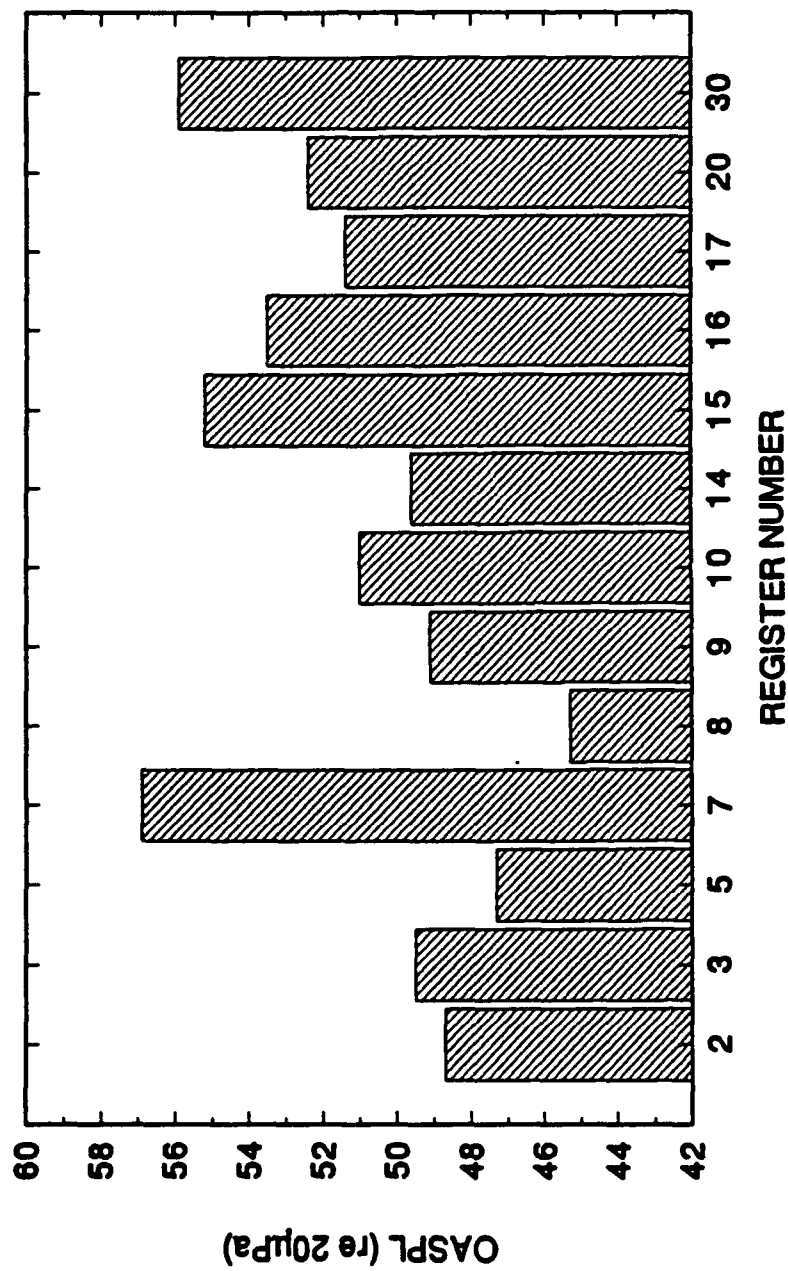
Figure 4.1   OASPL Measured at 4.66 m/s for Each Register.
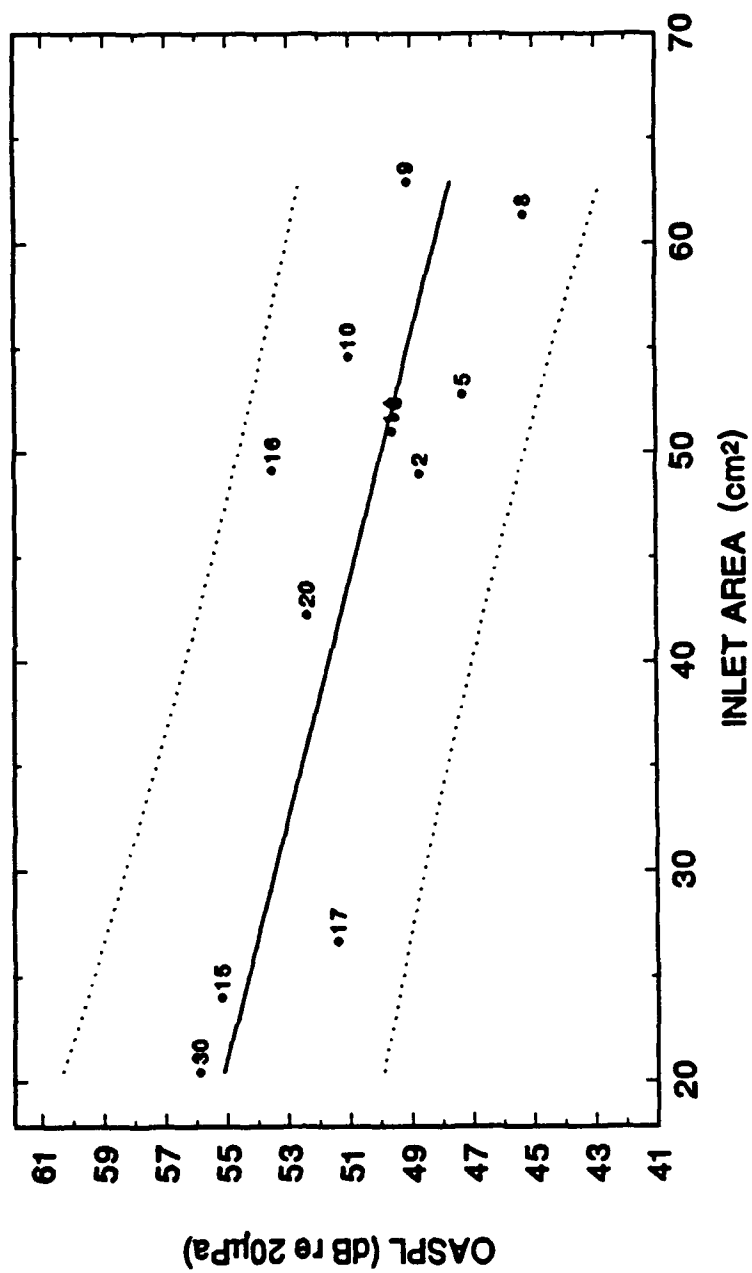
Figure 4.2   OASPL at 4.66 m/s for Each Register vs. Inlet Area
(with 95% Confidence Bands).
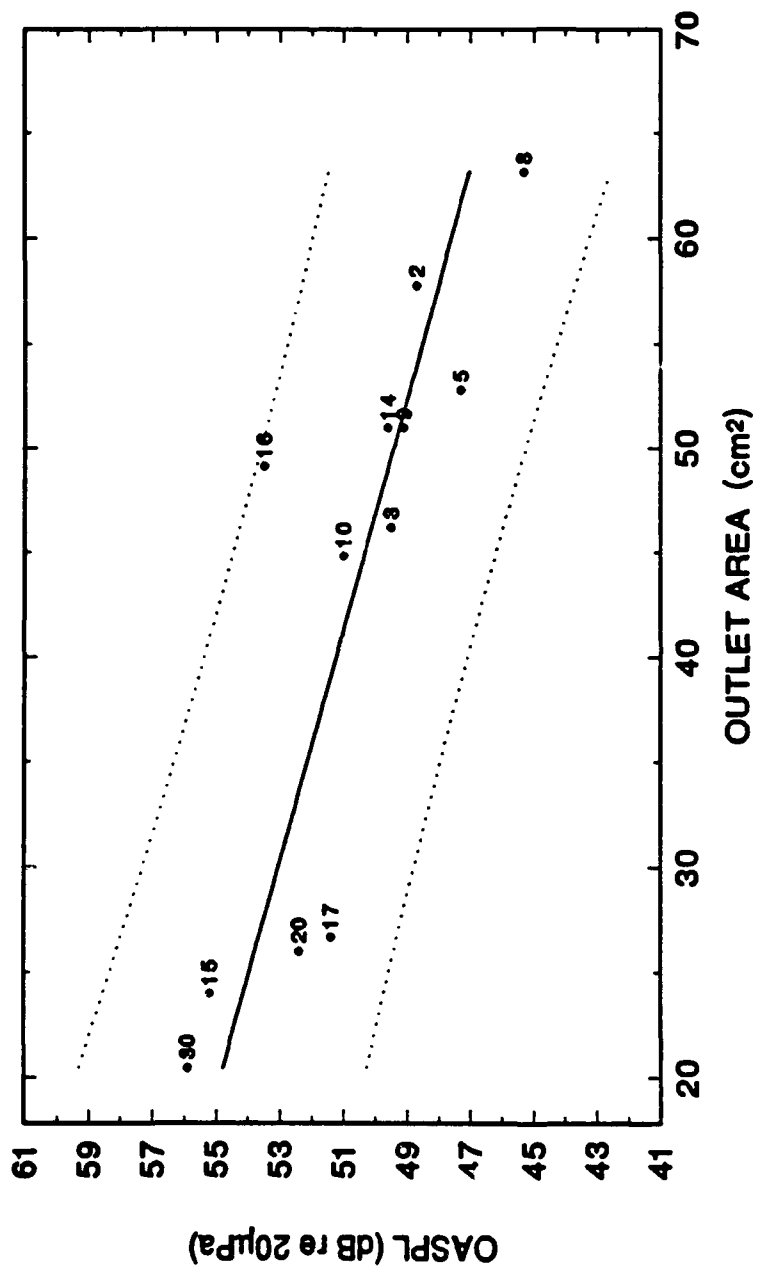
Figure 4.3   OASPL Measured at 4.66 m/s for Each Register vs. Outlet Area (with 95% Confidence Bands).

77
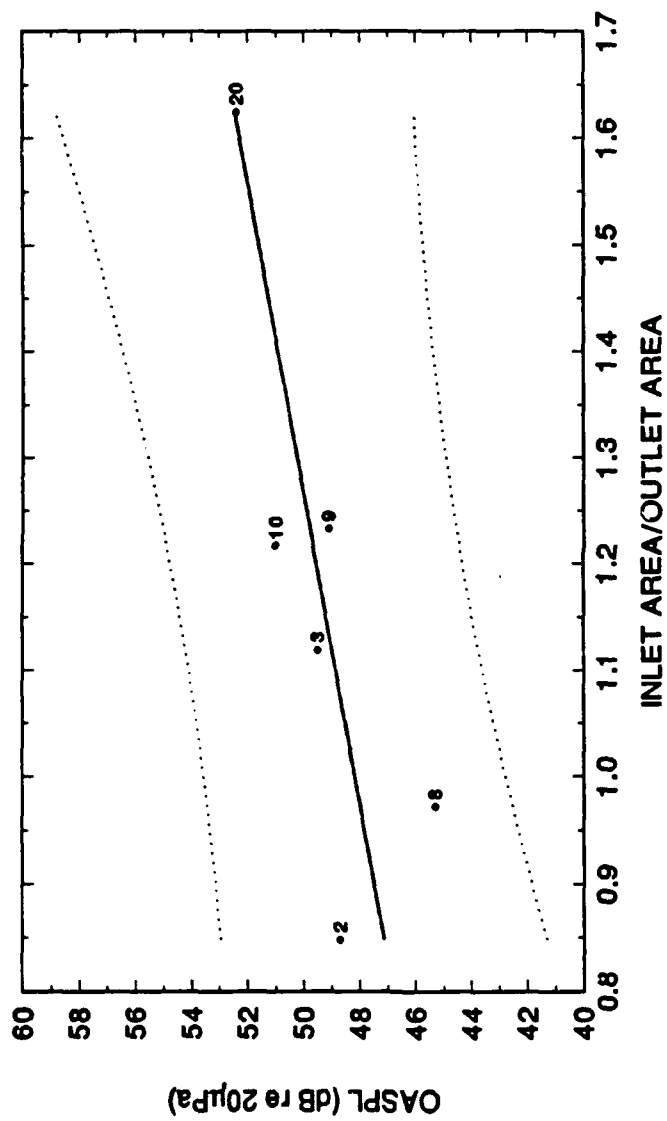
Figure 4.4   OASPL at 4.66 m/s for Each Register vs. Ratio of Inlet Area to Outlet Area (with 95% Confidence Bands).
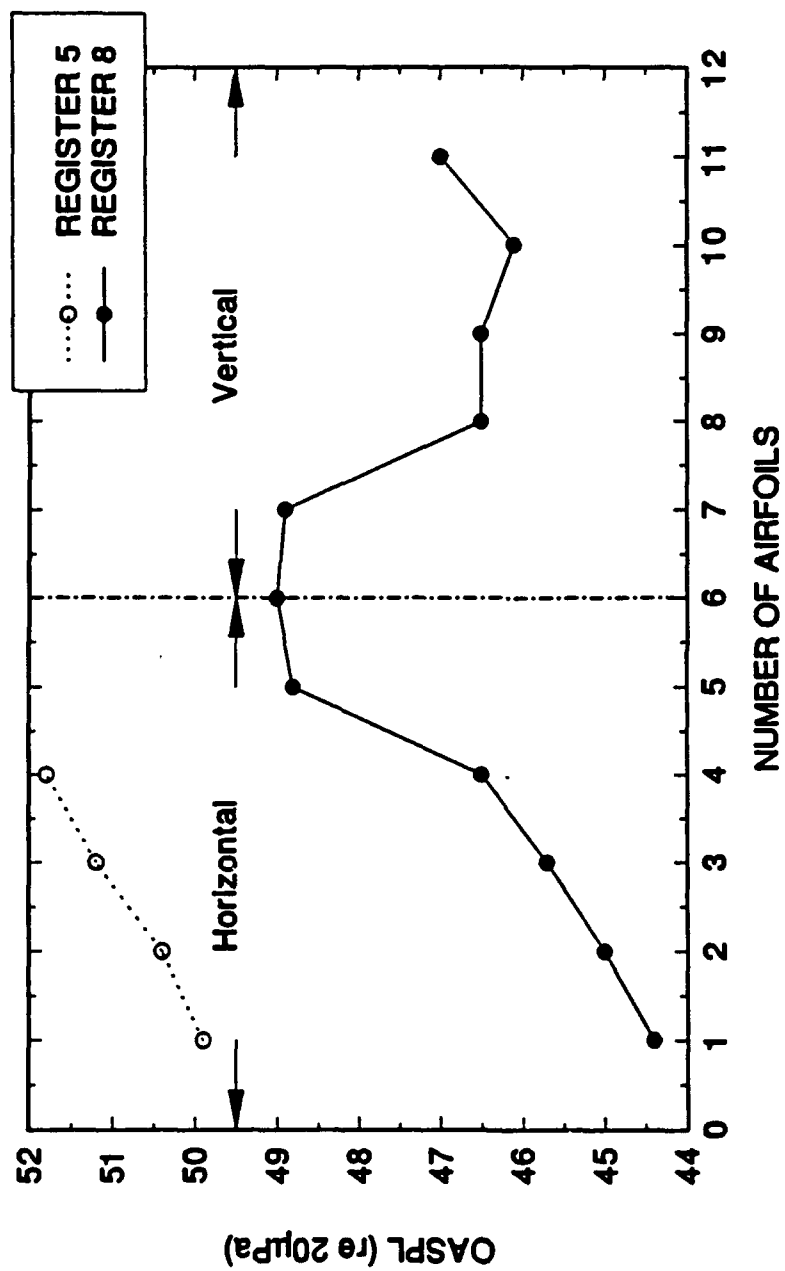
Figure 4.5   OASPL Measured at 5.26 m/s vs. Number of Vanes - Register 5 and 8.

The shut-off door is an apparent source of a low frequency, velocity dependent peak for registers 3 and 20. These peaks collapse to a Strouhal Number between 0.20 and 0.22 calculated using the thickness of the door. This is consistent with the work done on plates by Sieverding and Heinemann.[10] They show that vortex shedding of subsonic laminar flow over both sides a flat plate, with a square trailing edge, scales to a Strouhal number of 0.215.

Chapter 5

CONCLUSIONS AND RECOMMENDATIONS

5.1 Conclusions

The airfoils mounted in the louver housing radiate more intensely than the jet alone owing to the dipole mechanisms of flow over surfaces with free edges. On the average, a sixth power dependence of this dipole noise on flow velocity was found. Physical changes to the leading and trailing edges of these blades does not appreciably alter the power law dependence, but it may alter the level of radiation.

When individual blades are added one at a time to make up a louver vent, as demonstrated with registers 5 and 8, the noise increases in proportion to the number of airfoils ($N^{2/5}$). The addition of support struts tends to reduce the OASPL. These struts decorrelate the local pressure fluctuations along the trailing edge, making the trailing edge of the airfoils a less efficient radiator of sound.

Rearward and forward facing steps molded into individual blades are predominant sources of radiated sound. By removing them, 3 to 6 dB noise reduction may occur (register 5).

Inlet and outlet area has a definite effect on the radiated noise level. A small inlet or outlet area increases the velocity over the louvers resulting in higher radiated noise levels. If the outlet area is smaller than the inlet area (i.e. the ratio of inlet

80

area to outlet area is greater than 1.00), the OASPL is increased. This is also due to the increase in velocity over the blades.

Shut-off doors can cause an increase in low frequency noise levels that consistently scale on a Strouhal Number of 0.2 based on the thickness of the door. This is consistent with flat plate experimental data.[10]

5.2 Recommendations

Investigation into trailing edge shapes known to affect the radiation of sound from the trailing edge needs to be completed. A beveled trailing edge is geometrically simple and known to destabilize the wake vortex.[11] Recent analytical work has shown that the intensity of the radiated sound from an airfoil can be attenuated by having sawtooth or sinusoidal trailing edges.[12] This is achieved by effectively reducing the spanwise length of the trailing edge.

The effects of inflow turbulence on the radiated sound pressure level (turbulence ingestion) needs to be looked at in detail because in automotive applications, the registers are placed at HVAC duct terminations where free-stream turbulence is expected to be present. If inlet turbulence is found to dominate the noise emissions, then leading edge modifications may also be required.

The recommended elements of a quiet register would include: (1) the use of smooth airfoil shapes with sharp edges, (2) the addition of two or more vertical struts to ensure the decorrelation of trailing edge pressure fluctuations, and (3) design the inlet/outlet area for decelerating flow.

REFERENCES

1.   Brooks, T.F., Pope, D.S., and Marcolini, M.A. "Airfoil Self-Noise
      and Prediction," *NASA* Reference Publication 1218, July 1989.

2.   Ffowcs Williams, J.E. and Hall, L.H. "Aerodynamic Sound Generation by
      Turbulent Flow in the Vicinity of a Scattering Half Plane," *Journal of
      Fluid Mechanics* **40**, 1970, pp. 657-670.

3.   Blake, W.K. and Gershfeld, J.L.   "The Aeroacoustics of Trailing Edges,"
      Lecture Notes in Engineering, Frontiers in Experimental Fluid Mechanics
      (Gad-el-Hak, M., ed), Springer-Verlag; Berlin, **46**, 1989, pp. 457-532.

4.   Marboe, R.C., Lauchle, G.C., and Kargus, W.A.   "Quiet Wall Jet Facility
      for Basic Aero/Hydroacoustics Research,"   *ASME Book*   NCA, **10**
      (Farabee, T.M. and Arndt, R.E.A., eds.) 1991, pp 69-73.

5.   Bendat, J.S. and Piersol, A.G. *Random Data Analysis and Measurement
      Procedures*. J. Wiley & Sons, New-York, 1986.

6.   Neise W., "Acoustic Similarity Laws for Fans," *Journal of Engineering for
      Industry*, Transactions of the *ASME* **104**, pp. 162-168 (1982).

7.   Weidemann, J., "Analysis of the Relations Between Acoustic and
      Aerodynamic Parameters for a Series of Dimensionally Similar Centrifugal
      Fan Rotors," *NASA* Technical Translation, TT F-13,798, August 1971.

8.   Blake, W.K. *Mechanics of Flow Induced Sound and Vibration*, Vols. 1 and
      II, Academic Press, London, 1986.

9.   Lauchle, G.C. and Perry, L.A. "Aerodynamic Noise Generated by Cascaded
      Airfoils," Second International Congress on Recent Developments in Air
      and Structure-borne Sound and Vibration, March 1992.

10.   Sieverding, C.H. and Heinemann, H. "The Influence of Boundary Layer State
      on Vortex Shedding from Flat Plates and Turbine Cascades." *Journal of
      Turbomachinery*, **112**, April 1990, pp. 181-187.

11. Greenway, M.E. and Wood, C.J. "The Effect of a Bevelled Trailing Edge on Vortex Shedding and Vibration," *J. Fluid Mech.* (1973), **61**, part 2, pp. 323-335.

12. Howe, M.S. "Noise Produced by a Sawtooth Trailing Edge," *J. Acoust. Soc. Am.*,**90**(1), July 1991, pp. 482-487.

13. Mongeau, L. "Experimental Study of the Mechanism of Sound Generation by Rotating Stall in Centrifugal Trubomachines," Ph.D. thesis. The Pennsylvania State University, University Park, 1991.

Appendix

SPECTRAL DECOMPOSITION PROCEDURE

Strouhal effects are useful in the interpretation of noise data since they are related to the fluid mechanics rather than to the acoustic characteristics of the environment. The interpretation of noise spectra is simplified if the Strouhal effects can be extracted. A Fortran program was written to decompose the sound level spectra. A summary of this method and the Fortran code used is contained in this appendix. A detailed explanation of the procedure is contained in Reference 13.

An abbreviated description of the steps used in the procedure is provided below:

- Acquire sound level spectral densities at different inflow velocities.

- Plot the spectra keeping the Strouhal number constant. By the definition of the Strouhal number, there can be only one point from each spectrum. Constant Strouhal curves are produced from this step.

- Adjust the levels of the constant Strouhal curves to remove velocity dependence. This results in a G(He) function. The magnitude of this function is normalized by making the average value of 20log(G), along the lowest constant Strouhal curve, zero.

- Apply a goodness-of-fit estimate to smooth the resulting G(He) function.

- The F(St) functions are obtained by subtracting the smoothed G(He) function from each of the original spectra.

The Fortran code used in this experiment is presented below:

```
C*****************************************************************************
C
C     Collapse.for
C
C     This program decomposes the measured radiated noise into the acoustic
C     source strength function, F, and the acoustic frequency response
C     function, G.  Spectra from ten different RPM are decomposed in this
C     program.
C
C     Paul Bent     5/22/91           Orginal Program
C     Walt Kargus   5/08/92           Modified
C     L. A. Perry   6/08/92           Modified
C*****************************************************************************
C
C
      DIMENSION SF(10,1600),SST(10,1600),SHE(10,1600)
      DIMENSION SL(10,1600),SLA(10,1600),SLF(10,1600)
C**       DIMENSION RPM(10),BPF(10),VTIP(10)
      DIMENSION VEL(10)
      DIMENSION J1(10),J2(10)
      DIMENSION GHE(5000),GL(5000)
      DIMENSION GLS(500)
      DIMENSION CENBIN(500)
C
      CHARACTER*30 FNAME
      CHARACTER*30 GFUNC,GFUNCS,ADJLEV
      CHARACTER*30 SPECT1,SPECT2,SPECT3,SPECT4,SPECT5
      CHARACTER*30 SPECT6,SPECT7,SPECT8,SPECT9,SPECT0
      CHARACTER*30 FSPEC1,FSPEC2,FSPEC3,FSPEC4,FSPEC5
      CHARACTER*30 FSPEC6,FSPEC7,FSPEC8,FSPEC9,FSPEC0
C
      REAL*8 AREA1,AREA2,ATEMP1,ATEMP2
      REAL*8 DELAREA,SHIFT
C
C
C  INPUT CONSTANT DATA
C
C     A         SPEED OF SOUND                      m/s
C     D         DIAMETER OF THE IMPELLER            m
C     RHOO      STAGNATION AIR DENSITY              kg/m^2
C     PREF      REFERENCE PRESSURE                  Pa
C     Z         NUMBER OF IMPELLER BLADES
C
      DATA      A/340.0/
      DATA      RHOO/1.21/
      DATA      PREF/2E-5/
      DATA      PI/3.141592654/
      DATA      VEL/3.27,3.80,4.25,4.66,5.26,5.60,6.07,0.0,0.0,0.0/
C
C  READ INSTRUCTION FILE
C
      WRITE(*,*) 'PLEASE ENTER INSTRUCTION FILE NAME: '
      READ(*,255) FNAME
255   format(a30)
      write(*,*)'Enter in meters desired length scale:'
      read(*,*)D
```

```
          OPEN(UNIT=11,FILE=FNAME,STATUS='OLD')
          READ(11,*)  M,N,FMAX,RES,XMACH,HESET
          READ(11,*)   STSTART,STSTOP,STSTEP
          READ(11,96) GFUNC,GFUNCS
          READ(11,90) SPECT1,FSPEC1
          READ(11,90) SPECT2,FSPEC2
          READ(11,90) SPECT3,FSPEC3
          READ(11,90) SPECT4,FSPEC4
          READ(11,90) SPECT5,FSPEC5
          READ(11,90) SPECT6,FSPEC6
          READ(11,90) SPECT7,FSPEC7
C         READ(11,90) SPECT8,FSPEC8
C         READ(11,90) SPECT9,FSPEC9
C         READ(11,90) SPECT0,FSPEC0
      CLOSE(UNIT=11)
C
      WRITE(0,200)
  200 FORMAT(20X,'READING INSTRUCTION FILE')
C
C         DO 70 I=1,M
C         WRITE(0,*)RPM(I)
C 70      CONTINUE
C
C
          OPEN(UNIT=1,FILE=SPECT1,STATUS='OLD')
          OPEN(UNIT=2,FILE=SPECT2,STATUS='OLD')
          OPEN(UNIT=3,FILE=SPECT3,STATUS='OLD')
          OPEN(UNIT=4,FILE=SPECT4,STATUS='OLD')
          OPEN(UNIT=5,FILE=SPECT5,STATUS='OLD')
          OPEN(UNIT=6,FILE=SPECT6,STATUS='OLD')
          OPEN(UNIT=7,FILE=SPECT7,STATUS='OLD')
C         OPEN(UNIT=8,FILE=SPECT8,STATUS='OLD')
C         OPEN(UNIT=9,FILE=SPECT9,STATUS='OLD')
C         OPEN(UNIT=10,FILE=SPECT0,STATUS='OLD')
C
C  READ IN THE SPECTRA FREQUENCY (SF) AND LEVEL (SL) AT EACH RPM
C
      DO 2 I=1,M
      DO 1 J=1,N
          READ(I,*)SF(I,J),SL(I,J)
C         WRITE(0,*)SF(I,J),SL(I,J)
C
   1  CONTINUE
C
          WRITE(0,201)I,VEL(I)
  201     FORMAT(20X,'READING DATA FILE:',I4,5X,'VEL: ',F8.2)
C
   2  CONTINUE
C
      DO 42 I=1,M
          CLOSE(UNIT=I)
  42  CONTINUE
C
C  FIND THE BLADE PASSAGE FREQUENCY (BPF) AND TIP SPEED (VTIP) AT EACH RPM
C
C**       DO 3 I=1,M
C**          BPF(I)=RPM(I)*Z/60.
C**          VTIP(I)=RPM(I)*D*PI/60.
C
C         WRITE(0,*)I,BPF(I),VTIP(I)
C
   3  CONTINUE
C
C  GENERATE TWO NEW ARRAYS:  CHANGE FREQUENCY FROM Hz TO St AND He
C
      FACT = D/A
      DO 5 I=1,M
      DO 4 J=1,N
          SST(I,J)=SF(I,J)*D/VEL(I)
          SHE(I,J)=SF(I,J)*FACT
   4  CONTINUE
   5  CONTINUE
C
C  ADJUST THE LEVEL IN EACH SPECTRUM BY THE AMOUNT FROM THEORY
C
```

```fortran
C   CALCULTE THE DECIBEL OFFSET REQUIRED IN THEORY
C
c**         DELF=FMAX/REAL(N)
c wk- My definiition of the spl requires delf=1
c       DELF=SF(1,10)-SF(1,9)
        DELF=1
        DBOFF=10*ALOG10(RHOO*RHOO*D*DELF/PREF/PREF/(A**(XMACH)))
C
C       WRITE(*,*)DELF,DBOFF
C
        DO 7 I=1,M
        DO 6 J=1,N
           SLA(I,J)=SL(I,J)-10.*(3.+XMACH)*ALOG10(VEL(I))-DBOFF
C
C          WRITE(0,*)I,F,SL(I,J),SLA(I,J)
C
    6   CONTINUE
        VELOFF=10.*(3.+XMACH)*ALOG10(VEL(I))
C       WRITE(0,*)RPM(I),VELOFF
    7   CONTINUE
C
C       OPEN(UNIT=35,FILE=ADJLEV,STATUS='UNKNOWN')
C       DO 401 J=1,N
C       F=REAL(J)*1.5625
C       WRITE(35,*)F,SLA(I,J)
C401    CONTINUE
C       CLOSE(UNIT=35)
C
C   IN THIS SECTION, POINTS OF CONSTANT STROUHAL NUMBER
C   FROM SPECTRA OF DIFFERENT RPM WILL BE FOUND
C
C   SPECIFY STROUHAL NUMBER RANGE OF INTEREST
C
C       STSTART=0.35
C       STSTOP=4.0
C       STSTEP=0.025
C
C   SEARCH EACH SPECTRA FOR POINTS OF CONSTANT STROUHAL NUMBER
C
        ST=STSTART
        ITER=1
C
C       HELO1=ST*BPF(1)*D/A
C       HEHI1=ST*BPF(M)*D/A
C       HEMIN=HELO1
C
        DO 23 I=1,M
        J1(I)=1
        J2(I)=1
   23   CONTINUE
C
        DO 9 I=1,M
        DO 8 J=1,N
           IF(SST(I,J).GE.ST)GOTO 10
    8   CONTINUE
   10   J1(I)=J
    9   CONTINUE
C
        HELO1=SHE(1,J1(1))
        HEHI1=SHE(M,J1(M))
        HEMIN=HELO1
C
        DO 25 I=1,M
        GHE(I)=SHE(I,J1(I))
c       write(*,*)i,j1(i),she(i,j1(i)),ghe(i)
        GL(I)=SLA(I,J1(I))
```

```
     25  CONTINUE
C
         INDEX=M
C
C  INCREMENT THE STROUHAL NUMBER AND AGAIN SEARCH FOR POINTS OF
C  CONSTANT ST
C
         ST=ST+STSTEP
C
C 99  HELO2=ST*BPF(1)*D/A
C     HEHI2=ST*BPF(M)*D/A
C
     99  DO 12 I=1,M
         DO 11 J=1,N
             IF(SST(I,J).GE.ST)GOTO 13
     11  CONTINUE
     13  J2(I)=J
     12  CONTINUE
C
         HELO2=SHE(1,J2(1))
         HEHI2=SHE(M,J2(M))
C
C        DO 50 I=1,M
C        WRITE(0,*)ITER
C        WRITE(0,*)SHE(I,J1(I)),SLA(I,J1(I)),SST(I,J1(I))
C 50  CONTINUE
C        DO 51 I=1,M
C        WRITE(0,*)SHE(I,J2(I)),SLA(I,J2(I)),SST(I,J2(I))
C 51  CONTINUE
C
         IF(ITER.GT.1)GOTO 98
C
C  FIND AVERAGE ADJUSTED LEVEL OF THE DATA FOR LOWEST STROUHAL NUMBER
C
C        SUM = 0.
C        DO 14 I=1,M
C            SUM = SUM+SLA(I,J1(I))
C 14  CONTINUE
C
C        AVG = SUM/REAL(M)
C        OFFSET = AVG
C
C  COMPUTE THE AREA OF OVERLAP BETWEEN THE CURVES
C     -  USE TRAPEZOIDAL RULE  -
C
C
C  FIND AREA IN OVERLAP REGION UNDER LOWER ST CURVE
C
     98  AREA1=0.
         ATEMP1=0.
C
         DO 15 I=1,M
         IM1=I-1
         IF(SHE(I,J1(I)).EQ.HELO2)GOTO 17
         IF(SHE(I,J1(I)).GT.HELO2)GOTO 16
     15  CONTINUE
C
C  FIND AREA IN OVERLAP REGION UNDER LOWER STROUHAL CURVE
C
     16  CALL INTERP(SHE(IM1,J1(IM1)),HELO2,SHE(I,J1(I)),SLA(IM1,J1(IM1)),
        &              SLA(I,J1(I)),SLATEMP)
         ATEMP1=((SLATEMP+SLA(I,J1(I)))/2.)*(SHE(I,J1(I))-HELO2)
C
     17  DO 18 K=I,M-1
         KP1=K+1
         AREA1=AREA1+(SLA(K,J1(K))+SLA(KP1,J1(KP1)))/2.*(SHE(KP1,J1(KP1))
```

```
     &                  -SHE(K,J1(K)))
   18  CONTINUE
       AREA1=AREA1+ATEMP1
C
C  FIND AREA IN OVERLAP REGION UNDER INCREMENTED STROUHAL CURVE
C
       AREA2=0.
       ATEMP2=0.
       DO 19 I=1,M
       IM1=I-1
       IM2=I-2
       IF(SHE(I,J2(I)).EQ.HEHI1)GOTO 21
       IF(SHE(I,J2(I)).GT.HEHI1)GOTO 20
   19  CONTINUE
C
   20  CALL INTERP(SHE(IM1,J2(IM1)),HEHI1,SHE(I,J2(I)),SLA(IM1,J2(IM1)),
       &            SLA(I,J2(I)),SLATEMP)
       ATEMP2=((SLATEMP+SLA(IM1,J2(IM1)))/2.)*(HEHI1-SHE(IM1,J2(IM1)))
C
   21  DO 22 K=1,IM2
       KP1=K+1
       AREA2=AREA2+(SLA(K,J2(K))+SLA(KP1,J2(KP1)))/2.*(SHE(KP1,J2(KP1))
       &            -SHE(K,J2(K)))
   22  CONTINUE
       AREA2=AREA2+ATEMP2
C
C  CALCULATE THE AREA BETWEEN THE CURVES AND AMOUNT OF SHIFT
C
       DELAREA=AREA2-AREA1
       hehoff=hehi1-helo2
         if (hehoff.gt.0.0) then
            SHIFT=DELAREA/(HEHI1-HELO2)
         else
            SHIFT=DELAREA/1.0
         endif
       DBSHIFT=DBSHIFT+SHIFT
C
C      WRITE(0,*)AREA1,AREA2,DELAREA,SHIFT
C
C  ADJUST THE LEVEL OF THE HIGHER ST CURVE BY SHIFT AMOUNT
C  STORE RESULT IN ARRAY FOR G FUNCTION
C
       DO 26 I=1,M
       II=INDEX+I
       GHE(II)=SHE(I,J2(I))
       GL(II)=SLA(I,J2(I))-DBSHIFT
   26  CONTINUE
       INDEX=II
C
C  RESET VALUES BEFORE INCREMENTING TO NEXT STROUHAL NUMBER
C
       ITER=ITER+1
       HELO1=HELO2
       HEHI1=HEHI2
       AREA1=0.0
       AREA2=0.0
       ATEMP1=0.0
       ATEMP2=0.0
C
       DO 27 I=1,M
       J1(I)=J2(I)
   27  CONTINUE
C
       ST=ST+STSTEP
       IF(ST.LE.STSTOP)GOTO 99
C
```

```
C   THE LEVEL OF THE G FUNCTION HAS BEEN FOUND OVER THE FREQUENCY
C   RANGE OF INTEREST
C
C   SMOOTH THE G FUNCTION SO IT CAN BE SUBTRACTED
C   EASILY FROM THE ORIGINAL SPECTRA
C
C
    HEMAX=HEHI2
    DELHE=(HEMAX-HEMIN)/RES
C
C   WRITE(0,*)HEMIN,HEMAX,DELHE
C
C
C   IMAX IS THE NUMBER OF POINTS FORMING G FUNCTION
C   IBIN IS THE NUMBER OF HELMHOLTZ NUMBER BINS TO USE
C
    IMAX=INT(REAL(M)*(STSTOP-STSTART)/STSTEP)
    IBIN=INT(RES)
C
    BINLO=HEMIN
    ICOUNT=0
    SUM=0.0
C
    DO 40 J=1,IBIN
    GLS(J)=0.0
40  CONTINUE
C
    DO 29 J=1,IBIN
    BINHI=BINLO+DELHE
    DO 28 I=1,IMAX
C
C    WRITE(0,*)GHE(I),BINLO,BINHI
C
    IF(GHE(I).GE.BINLO.AND.GHE(I).LT.BINHI)THEN
                                ICOUNT=ICOUNT+1
                                SUM=SUM+GL(I)
                                END IF
28  CONTINUE
    IF(ICOUNT.EQ.0)THEN
                    GLS(J)=GLS(J-1)
                    CENBIN(J)=(BINLO+BINHI)/2.
                    GOTO 92
                    END IF
    CENBIN(J)=(BINLO+BINHI)/2.
    GLS(J)=SUM/REAL(ICOUNT)
C
C   WRITE(0,*)GLS(J)
C
92  BINLO=BINHI
    ICOUNT=0
    SUM=0.0
29  CONTINUE
C
C   THE SMOOTHED VALUE OF THE G FUNCTION HAS BEEN FOUND IN A
C   SPECIFIED NUMBER OF HELMHOLTZ NUMBER BINS
C
C   NOW FIX THE LEVEL OF THE G FUNCTION AT A SPECIFIED
C   HELMHOLTZ NUMBER
C
    DO 300 I=1,IBIN
C   WRITE(0,*)CENBIN(I),HESET
    IF(CENBIN(I).GE.HESET)THEN
                            OFFSET=GLS(I)
                            WRITE(0,311)OFFSET
311                         FORMAT(20X,'OFFSET:',1X,F12.3)
                            GOTO 302
```

```
                                        END IF
    300 CONTINUE
C
    302 DO 301 J=1,IBIN
        GLS(J)=GLS(J)-OFFSET
    301 CONTINUE
C
C  SUBTRACT THE SMOOTHED G FUNCTION FROM THE INITIAL SPECTRA
C  TO DETERMINE THE LEVEL OF THE F FUNCTION
C
C
C       WRITE(0,*)HEMIN,HEMAX
C
        WRITE(0,203)
    203 FORMAT(20X,'COMPUTING F FUNCTION')

        DO 30 I=1,M
        K=1
        HEBOT=HEMIN
        DO 31 J=1,N
        IF(SHE(I,J).LT.HEBOT)GOTO 31
        IF(SHE(I,J).GT.HEMAX)GOTO 30
    33  HETEMP=HEBOT+DELHE
        IF(SHE(I,J).GT.HETEMP)THEN
                                K=K+1
                                HEBOT=HETEMP
                                GOTO 33
                                END IF
        SLF(I,J)=SL(I,J)-10.*(XMACH+3.)*ALOG10(VEL(I))-DBOFF-GLS(K)
C     S            +OFFSET
C       WRITE(0,*)I,J,SLF(I,J)
    31  CONTINUE
    30  CONTINUE
C
    32  CONTINUE
C
C  THE LEVEL OF THE F FUNCTION HAS BEEN DETERMINED
C
C  WRITE OUTPUT TO DATA FILE
C
        OPEN(UNIT=12,FILE=GFUNC,STATUS='UNKNOWN')
        OPEN(UNIT=13,FILE=GFUNCS,STATUS='UNKNOWN')
C
C  FIRST WRITE ALL THE POINTS CONPRISING THE G FUNCTION ESTIMATE
C  ALSO SUBTRACT THE OFFSET FROM THE POINTS COMPRISING THE G FUNCTION
C
        DO 83 K=1,IMAX
        GL(K)=GL(K)-OFFSET
    83  CONTINUE
C
        DO 34 K=1,IMAX
        WRITE(12,*) GHE(K),GL(K)
    34  CONTINUE
C
C  WRITE THE SMOOTHED G FUNCTION
C
        IRES=REAL(RES)
        DO 35 I=1,IRES
        freg=cenbin(i) * a/d
        WRITE(13,*) freg,CENBIN(I),GLS(I)
    35  CONTINUE
C
C  WRITE EACH OF THE F FUNCTIONS
C
        OPEN(UNIT=21,FILE=FSPEC1,STATUS='UNKNOWN')
        OPEN(UNIT=22,FILE=FSPEC2,STATUS='UNKNOWN')
```

```
      OPEN(UNIT=23,FILE=FSPEC3,STATUS='UNKNOWN')
      OPEN(UNIT=24,FILE=FSPEC4,STATUS='UNKNOWN')
      OPEN(UNIT=25,FILE=FSPEC5,STATUS='UNKNOWN')
      OPEN(UNIT=26,FILE=FSPEC6,STATUS='UNKNOWN')
      OPEN(UNIT=27,FILE=FSPEC7,STATUS='UNKNOWN')
C     OPEN(UNIT=28,FILE=FSPEC8,STATUS='UNKNOWN')
C     OPEN(UNIT=29,FILE=FSPEC9,STATUS='UNKNOWN')
C     OPEN(UNIT=30,FILE=FSPEC0,STATUS='UNKNOWN')
C
      DO 36 I=1,M
      DO 37 J=1,N
         IOPEN=20+I
         IF(SST(I,J).LT.STSTART)GOTO 37
         IF(SST(I,J).GT.STSTOP)GOTO 36
         WRITE(IOPEN,*)SF(I,J),SHE(I,J),SST(I,J),SLF(I,J)
   37 CONTINUE
   36 CONTINUE
C
C
      CLOSE(UNIT=12)
      CLOSE(UNIT=13)
C
      DO 41 I=1,M
         ICLOSE=20+I
         CLOSE(UNIT=ICLOSE)
   41 CONTINUE
C
C  FORMAT STATEMENTS
C
   90 FORMAT(5X,2A20)
   96 FORMAT(5X,2A20)
C100 FORMAT(1X,F7.2,9X,F6.3)
  100 FORMAT(5X,F10.3,10X,F10.3)
C
      STOP
      END
C
C
      SUBROUTINE INTERP(A,B,C,D,E,F)
C
C  THIS SUBROUTINE IS FOR LINEAR INTERPOLATION OF DATA
C  F IS THE VALUE TO BE INTERPOLATED FOR, A,B,C,D AND E ARE KNOWN
C
C                        A    D
C                        B    F
C                        C    E
C
      F=E+(B-C)*(D-E)/(A-C)
      RETURN
      END
```